

# CHALMERS



## A critical review of bending wave loudspeaker technology and implementation

Master's Thesis in the Master's programme in Sound and Vibration

**KUONAN LI**

Department of Civil and Environmental Engineering  
*Division of Applied Acoustics*  
*Room Acoustics Group*  
CHALMERS UNIVERSITY OF TECHNOLOGY  
Göteborg, Sweden 2010  
Master's Thesis 2010:9



MASTER'S THESIS 2010:9

# A critical review of bending wave loudspeaker technology and implementation

Master's Thesis in the Master's programme in Sound and Vibration

KUONAN LI

Department of Civil and Environmental Engineering  
*Division of Division of Applied Acoustics*  
*Room Acoustics Group*  
CHALMERS UNIVERSITY OF TECHNOLOGY  
Göteborg, Sweden 2010

A critical review of bending wave loudspeaker technology and implementation  
Master's Thesis in the Master's programme in Sound and Vibration  
KUONAN LI

© KUONAN LI, 2010

Master's Thesis 2010:9

Department of Civil and Environmental Engineering  
Division of *Division of Applied Acoustics*  
Room Acoustics Group  
Chalmers University of Technology  
SE-412 96 Göteborg  
Sweden  
Telephone: + 46 (0)31-772 1000

Department of Civil and Environmental Engineering  
Göteborg, Sweden 2010

A critical review of bending wave loudspeaker technology and implementation

Master's Thesis in the Master's programme in Sound and Vibration

KUONAN LI

Department of Civil and Environmental Engineering

Division of Applied Acoustics

Room Acoustics Group

Chalmers University of Technology

## ABSTRACT

The interest in flat panel loudspeakers has increased in recent years that various forms of bending wave loudspeakers (BWL) and distributed mode loudspeaker (DML) are of great interest to loudspeaker producers and have been developed for many different applications. Both BWL and DML are based on the use of bending waves. The main difference is that the BWL uses an infinite plate approach while the DML uses a finite plate approach, or preferably, a modal approach.

An introduction to these technologies is given in the beginning of this thesis. Then follow the bending wave theories, including famous Euler-Bernoulli beam equation, Kirchhoff plate theory and the corrections for these two simple cases. The elementary radiators that can be used for describing different approaches will be shown, as well as several particular concepts relevant to the measurements and simulations.

Afterward, some commercial products applying bending wave theories are discussed: the Bending Wave Loudspeaker from Göbel, the DDD driver from German Physiks, the sound transducer from Manger, and the commercially most important, the DML from NXT. The first three use an infinite plate approach while the last one is based on modal approach.

In order to study the relative performance of a DML, a sample provided by NXT is used as together with a conventional electro-dynamic. The two speakers are subject to a series of measurements, such as impulse response - which also implies frequency response - , directivity, sound power, efficiency, sensitivity, and nonlinear distortion. In addition, sound pressure levels are measured at 30 positions in a listening room to study sound distribution. The mechanical properties of the DML, including density, Young's modulus and mechanical impedance are vital for further simulation; therefore they are measured as well. A blind listening test is also done to investigate the listeners' responses to DML and the preference between DML and electrodynamic loudspeaker tested earlier.

At the end of the project, some simulations are carried out to optimize DML performance. The ratio of length to width is important for the distribution modes in frequency, as well as for choosing the optimum position of the exciter. Finally, finite element methods are employed using of Comsol's Mutiphysics software to investigate the effect of panel's size to sound pressure response at low frequencies. Also, the boundaries of the plate are varied as roller, free, or fixed in Comsol's model, to see how boundary conditions influence the frequency response.

With the result of the experiments mentioned above, one can conclude that DML has lower sensitivity and efficiency than the conventional electrodynamic loudspeaker tested here. The DML lack of low frequency is due to low modal density and the lack of high frequency is due to the transition of bending waves to transverse waves. The directivity of the DML is not better than the electrodynamic loudspeaker's in fact it measured less at mid-frequencies. The result of the simulations is that the best length/width ratio is between 0.95~0.99, depending how the optimum is defined.

Key words: bending wave loudspeaker, distributed mode loudspeaker, electrodynamic, electromagnetic, DML, BWL, NXT, Manger, German Physiks, DDD driver, Göbel

## Acknowledgements

This study journey in Sweden is exciting, surprising and fascinating. I have learned a lot more than I could imagine before my departure from Taiwan.

First of all, I would like to thank my supervisor, Professor Mendel Kleiner for giving me the opportunity to work in such an interesting topic. I have learned a great deal from discussion with him and my thinking are greatly inspired by him. Many thanks to his generous offer of time and advice to me during the period of thesis work. They are indispensable to the completeness of this project.

I also want to thank Börje Wijk for assisting me to use all types of instruments and helping me to set up for the measurement. I also want to appreciate Gunilla Skog for paper works. In addition, I'd like to thank the other teaching staff, including Professor Wolfgang Kropp, Dr. Patrik Andersson, Dr. Stig Kleiven, Dr. Astrid Pieringer and many others, for giving such good lectures and being so patient in guiding us during the master degree studies. I also wish to thank the other students of 2007, especially Chiao-Li Ling, Edmundo Guevara, Julia Winroth and Lennart Bureniv, for being more than just nice friends but also good mentors. Special thanks are due to Patrik Andersson for pointing out some problem in the thesis presentation and answering my questions in vibroacoustics.

The last but the most significant people I would like to thank are my families, including my parents, my sisters, my brother, my parents-in-law, and my sisters-in-law. A special thank to my dearest wife, Kai-Yi Hsu. Without you, I will never achieve so far.



# Contents

ABSTRACT	I
ACKNOWLEDGEMENTS	III
CONTENTS	V
1 INTRODUCTION	1
2 BENDING CHARACTERISTIC AND RADIATION	3
2.1 Introduction to bending wave	3
2.2 Bending wave equation	4
2.2.1 Euler-Bernoulli beam equation and near field	4
2.2.2 Dispersive	7
2.2.3 Kirchhoff theory for plates	8
2.2.4 Correction for Bending Waves Theories	9
2.3 Mode behaviour	9
2.4 Radiation	11
2.4.1 Monopole	12
2.4.2 Infinite plate radiation	13
2.4.3 Finite plate	16
3 DESIGN OF BENDING WAVE LOUDSPEAKERS	19
3.1 The Bending Wave Loudspeaker of Göbel	19
3.2 The DDD driver of German Physiks	20
3.3 The Sound Transducer of Manger	22
3.4 The Distributed Mode Loudspeaker of NXT	23
3.4.1 Introduction	23
3.4.2 Acoustic analogous circuit	23
3.4.3 Frequency response and polar response	25
3.4.4 Sound power	26
3.4.5 Excitation point, material of panels, and geometry of panel	26
4 PERFORMANCE OF LOUDSPEAKERS	29
4.1 Introduction to the test samples	29
4.2 Material properties	30
4.3 Impulse response and frequency response	34
4.4 Directivity	35
4.5 Radiated Sound Power, Efficiency, and Sensitivity	36

4.5.1	Diffuse method for sound power	36
4.5.2	Efficiency	38
4.5.3	Sensitivity	39
4.6	Distortion	39
4.7	Test on the Diffuse Sound of DML	41
4.8	Sound Pressure Level Distribution	42
4.9	Mechanical impedance	45
4.10	An example of a commercial DML exciter	48
4.11	Listening test	48
4.12	Diaphragm Scan	50
5	SIMULATION AND OPTIMIZATION	53
5.1	Optimization of length / width ratio	53
5.2	The dimension's effect to DML at low frequency	54
5.3	The boundaries effect to DML	55
5.4	DML model using measured material properties	56
6	CONCLUSION	57
7	SUGGESTION FOR FUTURE WORK	59
	BIBLIOGRAPHIC	61
	APPENDIX A1. QUESTIONNAIRE FOR LISTENING TEST	65
	APPENDIX A.2. INFORMATION OF SUBJECTS	68
	APPENDIX B. EQUIPMENT LIST	68
	APPENDIX C. MATLAB SCRIPTS	73
	APPENDIX D. PHOTOS	75

# 1 Introduction

Loudspeakers are commonly used for sound reproduction. They vary quite differently in sizes, types, shapes, and also as regards their working principles. Due to the distinct advantage of using less space, panel loudspeakers have become widely used in many applications, ranging from small loudspeakers embedded in cell phones to large loudspeakers for stereo systems. Bending wave loudspeakers have recently become an important type of flat loudspeakers. In addition to the distinct merit of space-saving properties, bending wave loudspeakers also have some exclusive acoustic characteristics; the most significant ones would be that they usually help excite diffuse sound fields and that they have low directivity even at high frequencies. Some commercial companies even claim that their products have directivity similar to a point source, i.e. omnidirectional [1]. In addition, it is also reported that some bending wave loudspeakers are able to radiate sound covering the full audio frequency range except for very low bass [2]. Therefore an extra tweeter and/or super-tweeter would become unnecessary for these products, while tweeters and sub-woofers are commonly used for conventional piston-like electro-dynamic loudspeakers in order to improve the reproduction of very low and high frequencies.

So far, it seems like bending wave loudspeakers have many advantages, but some questions emerge after showing these positive sides: if they are as good as they claim, why are there so few commercial high-quality loudspeakers using bending wave principles? Are these so called “Bending Wave Loudspeakers” really using bending wave to reproduce sounds? Is there any fatal weakness of these bending wave loudspeakers?

This thesis aims to investigate the construction principles and properties of bending wave loudspeakers, and will hopefully be able to answer the questions raised above. Nevertheless, it is necessary to have a good understanding of the fundamental characteristics of bending waves before reviewing bending wave loudspeakers. Thus basic bending wave theories will be the main concern of following chapter.

Generally speaking, unlike longitudinal waves and transverse waves, bending waves have a special property of having a sound speed that depends on frequency. Such waves are called “dispersive”. It is also necessary to always consider near fields when talking about bending waves, especially as regards vibration close to the excitation point and discontinuities. The most important property of any loudspeaker is its sound radiation. Without radiation, sounds would never be generated. Modal theory will be presented at the end of Chapter 2 as well.

Chapter 3 will discuss several commercial applications of bending wave loudspeakers. The structure and the working theories for them will also be studied. One of these loudspeakers, the so-called “Distributed Mode Loudspeaker”, has been studied considerably since its introduction in 1997. The function of this type of loudspeaker is based on resonant bending wave systems, so it also uses a modal approach.

In Chapter 4, a Distributed Mode Loudspeaker (DML) will be used as the test sample. Its mechanical and acoustic properties are measured in order to understand the product. These properties include the mechanical impedance of a given DML’s plate, the directivity, the vibration velocity, and the radiated power. They will be measured by means of accelerometer/force transducer, laserdoppler-vibrometer (LDV), and the diffuse field method for sound power. Furthermore, harmonic

distortion will be studied, as well as the sound pressure level distribution by the loudspeaker in a well-damped listening room; the lecture room at Applied Acoustics Division at Chalmers University of Technology. For comparison, a conventional electro-dynamic loudspeaker will be also used through the tests mentioned above, except those involving the properties of the diaphragm to illustrate the differences. The outcomes of the experiments will be shown in Chapter 4 and further studied.

At the end of Chapter 4, instead of analyzing its characteristics from the engineer's point of view, subjective listening tests will be carried out to see lay people's responses to DML. Five test sounds are used for the tests, including speech, drums, cello, piano and symphony. These sounds are generated by convolving the impulse responses of the two speakers with anechoically recorded music clips. Ten male and ten female subjects, age 20 to 30, participated this listening test. The test results are presented in accordance with the type of music, the gender of subjects, and so on. Possible explanation to this result and the pros and cons in psychoacoustics of using bending wave loudspeakers will be given.

As one can infer, the performance of DMLs can be optimized in several ways, including the length / width ratio, the position of the exciter(s), and the ratio of bending stiffness to the mass per area, in order to achieve different objectives, such as the best omnidirectional performance, the most evenly distributed modal density, and so on. The optimization process will be presented in Chapter 5. FEM models of the DML are also implemented to show how the size of the panel influences low frequency response and how the boundary conditions affect the response.

## 2 Bending characteristic and radiation

### 2.1 Introduction to bending wave

It is intuitive to discuss bending waves and their special properties since this thesis concerns about loudspeakers applying bending wave approaches. Hence, the classic Euler-Bernoulli beams theory, Kirchhoff plates theory are presented to help one understand these physical characteristics of bending waves.

In solids, longitudinal waves can occur, as well as in liquids and gases. They have well-known property that the particles' vibrations are along or parallel to the direction of waves' propagation. It is also possible to find the excitation of transverse waves in solids due to the presence of shear force; however, transverse waves hardly present in the media other than solid, i.e. liquids and gases. That is mainly because the particles in other media cannot resist in shape deformation as the particles of solid.

Apart from these two types of waves mentioned above, there is another sort of waves which is paramount of all various wave types in solids, especially while dealing with structure-borne sound and sound radiation of structures. They are so-called bending waves, also called flexural waves sometimes. They are significant not merely because of that they are one of the most common types of waves in solids, but also due to the fact that sound radiation are mainly contributed by them, that is due to the fact that the displacements of bending waves are perpendicular to the directions of propagations and this nature means bending waves lead to much more interactions between the structures and the adjacent medium, e.g. the most common one, air, than the other waves do. Thus most of the energy transmitted to the adjacent medium is by means of bending waves, i.e. bending waves are majorly responsible to radiations. But before discussion of radiation, one should understand the characteristics of flexural waves as the first thing.

The following subsections will give a tour of the features of bending waves, starting with the most prominent and significant Euler-Bernoulli one-dimensional theory, following the Kirchhoff theory for plates. By demonstrations of these two theories, it is sufficient to unveil the basic properties of flexural waves. One of the most important is the "dispersive" nature of bending wave speed; nevertheless, the excitation of bending wave near field has the same importance.

However, both theories employ the assumption of non-deformable cross section, therefore erroneous results are expectable at high frequencies. To compensate this shortcoming, Timoshenko and Mindlin had developed their theories respectively. In spite of they are still limited, they gives relatively accurate outcomes at high frequencies. The details of these corrections will be neglected, instead, only the considerations one should note before applying these corrections will be introduced.

Afterward, one needs to know the mechanical impedance of the vibrating structures, especially the driving point impedance, occasionally also called point impedance for short. With this knowledge of point impedance, one can derive the vibration of the excitation point from a given excitation force.

By the end of this chapter, the modal approach will be brought in and the unique orthogonal feature of modes will be shown. In the last subsection, the fundamental sound radiators, consisting of monopole, infinite plates, and finite plates will be surveyed. One will see the significance of the flexure near field here and the critical frequency  $f_c$ .

## 2.2 Bending wave equation

### 2.2.1 Euler-Bernoulli beam equation and near field

Let's start with considering a slim beam with thickness and height much shorter than length. While it is under excitation, longitudinal wave and transversal wave often appear at the same time, which respectively represent compressions and lateral deflections. Bending waves also show these two behaviours simultaneously, thus it has been often misunderstood as the combination of longitudinal waves and transverse waves. Nevertheless, bending wave does not fall into any group of them. Instead, it belongs to the group of itself. Due to the property of showing compressions and lateral deformations at the same time, bending wave must be presented by four variables, while two variables are enough to describe longitudinal wave and transverse wave. These four parameters respectively are: transverse velocity  $v_y$ , angular velocity  $\omega_z$ , bending moment  $M_z$ , and shear force  $F_y$ . These four variables are related by four equations and therefore need four boundary conditions to solve the equations.

Assume that the cross sections of the beam remain still while under bending. Figure 2.1 illustrates the displacement and deformation in bending.

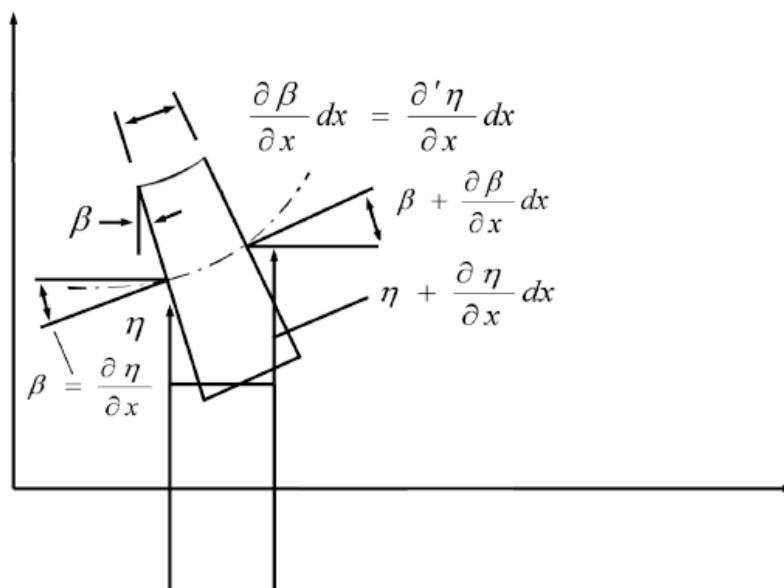


Figure 2.1: The displacement and deformation in bending.[3]

By observing Figure 2.1, one can infer the relation between vertical displacement  $\eta$  and rotation angle  $\beta$ .

$$\beta = \frac{\partial \eta}{\partial x} \quad (2.1)$$

The derivative of Eq (2.1) with respect to time will lead to following expression of angular velocity  $\omega_z$  and lateral velocity  $v_y$ :

$$\omega_z = \frac{\partial v_y}{\partial x} \quad (2.2)$$

Again, differentiate Eq (2.2) with respect to x-axis, yielding:

$$\frac{\partial \omega_z}{\partial x} = \frac{\partial^2 v_y}{\partial x^2} = \frac{\partial}{\partial t} \left( \frac{\partial^2 \eta}{\partial x^2} \right) \quad (2.3)$$

The last term of the above equation is the curvature of the bending, which is proportional to the bending moment  $M_z$  and inverse proportional to the bending stiffness  $B$ :

$$\frac{\partial^2 \eta}{\partial x^2} = -\frac{M_z}{B} \quad (2.4)$$

The bending stiffness  $B$  is defined as  $B = EI$ .  $E$  is the Young's modulus of the beam and  $I$  the moment of inertia of the beam. In the case of beam with rectangular cross section with height  $h$  and width  $b$ ,  $I$  is:

$$I = \frac{bh^3}{12} \quad (2.5)$$

Assume the cross section of beam remains un-deformable while the beam is bent. Figure 2.2 illustrates the cross section of a beam with moment  $M_z$  and shear force  $F_z$  acting on it.

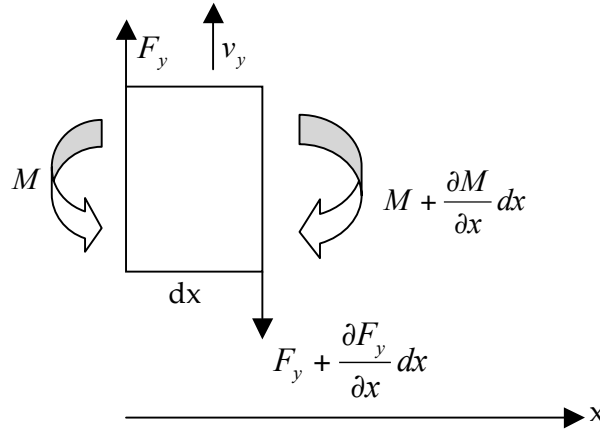


**Figure 2.2: a cross section of a beam with moment  $M_z$  and shear force  $F_z$  acting on it.**

In steady state, the total moment must be balanced; therefore one can derive  $F_z$  by means of the negative partial differentiation of the moment with respect to x-axis, i.e.

$$F_z = -\frac{\partial M_z}{\partial x} \quad (2.6)$$

Express  $M_z$  by Eq (2.4) and insert it into the above equation, it becomes:

$$F_z = -B \frac{\partial^3 \eta}{\partial x^3} \quad (2.7)$$

Additionally, in Figure 2.2, Newton's second law of motion gives:

$$F_z = -m \frac{\partial v_y}{\partial t} = -m \frac{\partial^2 \eta}{\partial t^2}$$

Or

$$\frac{\partial F_z}{\partial x} = -m' \frac{\partial^2 \eta}{\partial t^2} \quad (2.8)$$

where  $m'$  is the mass per unit length of the beam (along x-axis), which can be expressed by the density of the beam  $\rho$  as:

$$m' = \rho wh \quad (2.9)$$

Insert Eq (2.7) into Eq(2.8), the one-dimension bending wave equation is obtained,

$$B \frac{\partial^4 \eta}{\partial x^4} = -m' \frac{\partial^2 \eta}{\partial t^2}$$

which is more often presented in the form of:

$$B \frac{\partial^4 \eta}{\partial x^4} + m' \frac{\partial^2 \eta}{\partial t^2} = 0 \quad (2.10)$$

Eq (2.10) is well-known as the ‘‘Euler-Bernoulli beam equation’’.

To solve this partial differential equation, one can use the expression of the displacement in the form of simple harmonic motion, such as:

$$\eta(x, t) = \hat{\eta} \cdot e^{-jk_B x} e^{j\omega t} \quad (2.11)$$

where  $\omega$  the angular frequency,  $k_B$  the wave number of the bending waves, defined as  $k_B = 2\pi/\lambda_B = \omega/c_B$ , where  $\lambda_B$  the wave length of bending waves,  $c_B$  the wave speed of bending waves.

By the use of Eq (2.11), one will have a very simple expression for Eq (2.10):

$$B\omega^2 - m' k_B^4 = 0 \quad (2.11a)$$

which gives the four solutions of wave number  $k_B$  with two real and two imaginary ones:

$$k_B = \begin{cases} \pm k \\ \pm jk \end{cases} \text{ where } k = \sqrt{\frac{m' \omega^2}{B}} \quad (2.12)$$

With this expression of  $k_B$ , one can have the full solution as:

$$\eta(x, t) = (\hat{\eta}_+ e^{-jkx} + \hat{\eta}_- e^{jkx} + \hat{\eta}_{+j} e^{-kx} + \hat{\eta}_{-j} e^{kx}) e^{j\omega t} \quad (2.13)$$

The positive and negative signs respectively implies the wave propagate along positive and negative x-axis. The later two are with the subscript of j, which denotes that they are different from the first two in that they decay exponentially with distance. Such terms are called ‘‘flexure near field’’ or simply ‘‘near field’’, since they only appear near excitation points and discontinuities of the structures, and they do not propagate like waves so that the name uses field instead wave.

The four unknown displacement amplitude,  $\eta_+$ ,  $\eta_-$ ,  $\eta_{+j}$ , and  $\eta_{-j}$  can be determined if boundary condition are provided, e.g. simple support. Note that the phases of near

field are imaginary. In some case of boundary condition, near field may greatly reduced even vanish. The simple support is a good example for that.

## 2.2.2 Dispersive

By the definition of wave number and Eq (2.12), the bending wave speed  $c_B$  can be defined as

$$c_B = \sqrt[4]{\frac{B}{m'}} \sqrt{\omega}. \quad (2.14)$$

As one can observe, the bending wave speed  $c_B$  is frequency-dependent instead of being constant like sound in the air. Figure 2.3 shows the wave speed of bending waves in steel and glass based on Eq (2.14). The wave speed in air is also given for comparison.

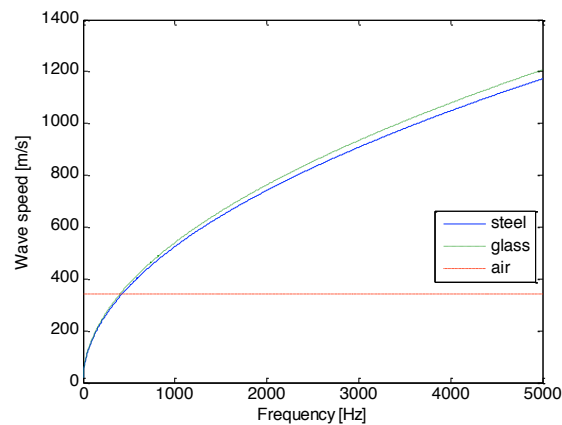


**Figure 2.3 Bending wave speeds of steel and glass versus frequency, along with the sound speed in air, where the beam of steel and glass have the same height  $h=3$  cm and width  $b=3$  cm. The temperature is  $20^\circ\text{C}$ . The material data:  $E_{\text{steel}}=200$  Gpa,  $\rho_{\text{steel}}=7850\text{kg/m}^3$ ,  $E_{\text{glass}}=72$  Gpa,  $\rho_{\text{steel}}=2520\text{kg/m}^3$ .**

By observing Eq (2.14), one can find the phase speed (the speed of sound) of bending wave is proportional to the square root of frequency, which means that at high frequencies, the bending waves travel much faster than the low frequencies. This property is called “dispersive”, which is carried from similar phenomenon in optics. It will result in unwanted distortion while transmitting a signal through a solid, because the high frequencies will reach the receiver much earlier than low frequencies do.

In addition, there seems no upper limit for bending waves’ speed in Figure 2.3. However it is not true because the simplification of non-deformable cross section will cause error at higher frequencies. As matter as fact, bending waves will change to transverse waves at higher frequencies, which gives the upper limit to wave speed.

Eq (2.14) can also be presented in the form related to the longitudinal waves’ speed [3] :

$$c_B \approx \sqrt{1.8c_L hf} = c_L \sqrt{\frac{1.8h}{\lambda}} \quad (2.15)$$

### 2.2.3 Kirchhoff theory for plates

As long as the propagation of plane bending wave is concerned, one must apply Kirchhoff's theory instead of Euler-Bernoulli theory; however, these two theories share the fundamental simplification, which is, the cross sections remain plane and perpendicular to the neutral line.

For a homogeneous plate placed on x-z plane of Cartesian coordinate, consider a wave travelling along with x-axis, Eq (2.10) must be modified as:

$$\frac{EI'}{1-\nu^2} \frac{\partial^4 \eta}{\partial x^4} + m'' \frac{\partial^2 \eta}{\partial t^2} = 0$$

where  $\nu$  is the Poisson's ratio,  $I'$  the moment of inertia of the plate, defined as  $I' = h^3/12$ , and  $m''$  the mass per unit area.

However, it is insufficient to describe a plate since the propagation along x-axis and z-axis may occur simultaneously. Hence it becomes:

$$B_x \frac{\partial^4 \eta}{\partial x^4} + B_{xz} 2 \frac{\partial^4 \eta}{\partial x^2 \partial z^2} + B_z \frac{\partial^4 \eta}{\partial z^4} + m' \frac{\partial^2 \eta}{\partial t^2} = 0 \quad (2.16)$$

where  $B_x$  and  $B_z$  are the bending stiffness in x-axis and z-axis direction, and  $B_{xz}$  is the bending stiffness for x-z axis, which is often approximated by  $B_{xz} = \sqrt{B_x B_z}$ . Since this plate is isotropic, therefore  $B_x = B_z = B_{xz} = EI'/1 - \nu^2 = B'$ .

Eq (2.16) seems very complicated at the first sight; however, as done in previous section, one can again surmise that the solution is in form of a harmonic wave, thus:

$$\eta(x, z, t) = \hat{\eta} \cdot e^{-j(k_x x + k_z z)} \cdot e^{j\omega t} \quad (2.17)$$

Substitutes Eq (2.17) into Eq (2.16) yielding:

$$\left[ B' (k_x^4 + 2k_x^2 k_z^2 + k_z^4) - m' \omega^2 \right] \hat{\eta} = 0$$

Or

$$B' (k_x^2 + k_z^2)^2 = m' \omega^2 \quad (2.18)$$

If one writes  $k_B^2 = k_x^2 + k_z^2$ , it will be nearly identical with one-dimension case, refer to Eq (2.12). Thus

$$k_B = \sqrt{\frac{\omega^2 m''}{B'}} \quad (2.19)$$

The difference between Eq (2.12) and Eq (2.19) is that for a plate the bending stiffness for plate  $B'$  is used instead of  $B$ , and the mass per unit area  $m''$  is employed to place the mass per unit length  $m'$ . The bending waves propagate at an angle  $\theta = \arctan(k_z/k_x)$ . As one can expect, for a fourth order partial equation like Eq (2.16), the solutions are greatly more complicated, even for some simple geometries of the plate and boundary conditions. Therefore, Finite Element Methods are often used to give an analytic solution, as well as for modal analysis.

## 2.2.4 Correction for Bending Waves Theories

The previous two theories are valid only if the wavelength of bending wave is large compared to the dimension of the cross section, and the errors introduced by the simple assumption of still cross section is ignorable. However, it is not the case at high frequencies. In order to overcome this problem, some corrections for bending wave theories had been developed. Here the basic ideas of the most important two will be introduced, and by considering these, the errors of bending wave theories can be greatly reduced and make them become more general.

The first thing one need to consider is the rotational energy, which is not included in former subsections but as matter as fact it becomes more significant as frequency increases. One might include it by adding the rotatory inertia into Eq (2.1).

Another vital correction term, which is first pointed out by Timoshenko, is to take the deformation caused by the shear force acting on the cross section into account. The derivation is beyond the scope of this thesis therefore neglected here. One who is interested in details can look up Page 109-115 of [4]. The approximately phase speed after correcting is:

$$c_B = \sqrt[4]{\frac{B}{m'}} \sqrt{\omega(1 - 3.6(\frac{h}{\lambda})^2)} \quad (2.20)$$

By examining Eq (2.1) and (2.20), one can reason out that to achieve the errors- or the difference- between Eq (2.1) and Eq (2.20) less than 10%, the wavelength should be longer than six times of the thickness. This particular wavelength decides the upper limit frequency at which simplified theories can still work fine with reasonable errors.

## 2.3 Mode behaviour

Consider that waves are propagating on a finite beam with two ends. When the waves reach one of the ends, it will be partially or totally reflected. The reflected wave is different from the original wave in amplitude and phase. The reflection will interfere with the sent one, sometime even resulting in total cancellation if they have the same amplitude and are out of phase. On the other hand, at certain frequencies, the reflected waves are in phase with the emitted waves, leading standing wave patterns, which are often named nature modes or mode patterns. These frequencies are called nature frequencies or resonant frequencies, which can be simply inferred by the period of waves' travelling.

Assume the wave speed is  $c$ , and the length of the beam is  $l$ . The period  $T$  is then the time which the wave travels to one end, reflected to the other end, and finally reflected back to the excitation position, i.e.  $T=2l/c$ . The first nature frequency  $f_1$  is hence  $f_1=c/2l$ . Because every periodic process with frequency  $f_1$ , therefore it can be analyzed in terms of sinusoidal components with frequencies:

$$f_n = n \frac{c}{2l} \quad (2.21)$$

Figure 2.4 shows the first 3 mode patterns.

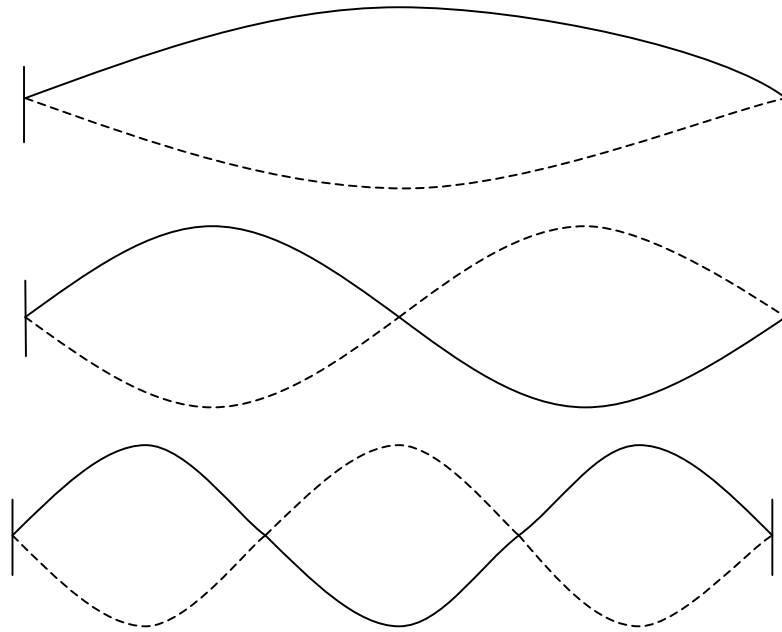


**Figure 2.4** The illustrations of the first 3 mode shape of a beam with both ends fixed.

As for bending waves, one can use Eq (2.14) for the wave speed in Eq (2.21), thus:

$$f_n = \sqrt{\frac{B}{m'}} \left( \frac{n\pi}{l} \right)^2 \quad (2.22)$$

For plates, it becomes

$$f_n = \sqrt{\frac{B'}{m''}} \left[ \left( \frac{n_1\pi}{l_x} \right)^2 + \left( \frac{n_2\pi}{l_y} \right)^2 \right] \quad (2.23)$$

where  $l_x$  the length of the plate,  $l_y$  the width of the plate.

When the given beam is excited by an impulse and set free, the beam will vibrate at these resonant frequencies. The modes corresponding to the resonant frequencies share a significant characteristic - being orthogonal to each other, which implies that one can expand the displacements or the velocity on any position of the structure to infinite numbers of modes. Consequently the kinetic energy will be the sum of the modes, making modes approach very powerful and commonly used for analysis.

The modes – or the eigenfunction – can be determined if the boundary conditions and the geometries of the structure under study are given. But if boundary conditions or the shapes of the device under study are complicated, e.g. an engine, one should seek for the help of software which employ finite elements method, such as Comsol Mutiphysics.

Take a simple support plate for example, which will be also used for the analysis in next chapter. The eigenfunctions of this case are:

$$\Phi_n(x, y) = \sin\left(\frac{n_1\pi x}{l_x}\right) \sin\left(\frac{n_2\pi y}{l_y}\right) \quad (2.24)$$

Assume the excitation is a point force, located at  $x_0, y_0$ . Using the modes expansion gives the modal force  $p_n$ .

$$p_n(\omega) = F_0(\omega) \sin\left(\frac{n_1\pi x_0}{l_x}\right) \sin\left(\frac{n_2\pi y_0}{l_y}\right) \quad (2.25)$$

, where  $F_0(\omega)$  the force response.

The normalization constant  $\Lambda_n$  is defined as:

$$\Lambda_n = \int_s m'' \Phi_n^2(x, y) dx dy \quad (2.26)$$

In this case, it is

$$\Lambda_n = \int_s m'' \Phi_n^2(x, y) dx dy = \int_s \rho h \sin\left(\frac{n_1\pi x}{l_x}\right) \sin\left(\frac{n_2\pi y}{l_y}\right) dx dy = \frac{\rho h l_x l_y}{4} \quad (2.27)$$

, where  $\rho$  is the density of the plate and  $h$  is the thickness.

Therefore, the velocity of any position can be expanded as:

$$v(x, y, \omega) = j\omega \sum_n \frac{p_n(\omega) \Phi_n(x, y)}{\Lambda_n (\omega_n^2 - \omega^2)} = j\omega \frac{4}{\rho h l_x l_y} \sum_n \frac{F_0(\omega) \sin\left(\frac{n_1\pi x_0}{l_x}\right) \sin\left(\frac{n_2\pi y_0}{l_y}\right) \sin\left(\frac{n_1\pi x}{l_x}\right) \sin\left(\frac{n_2\pi y}{l_y}\right)}{(\omega_n^2 - \omega^2)} \quad (2.28)$$

One may include the damping by adding the loss factor  $\eta$  into the denominator of the summation, making the equation more general. Thus Eq (2.26) becomes:

$$v(x, y, \omega) = j\omega \frac{4}{\rho h l_x l_y} \sum_n \frac{F_0(\omega) \sin\left(\frac{n_1\pi x_0}{l_x}\right) \sin\left(\frac{n_2\pi y_0}{l_y}\right) \sin\left(\frac{n_1\pi x}{l_x}\right) \sin\left(\frac{n_2\pi y}{l_y}\right)}{[\omega_n^2 (1 + j\eta) - \omega^2]} \quad (2.29)$$

The damping smoothes the peaks of the modes, but it also broadens the response given by each mode, resulting in a higher modal overlapping. Note that modal approach is only valid for the modal overlapping factor  $Q < 3$ , where  $Q$  value is defined as the number of resonance in certain modal bandwidth. The modal bandwidth is the frequency bandwidth starting from the frequency lower than the resonance frequency and at which frequency the amplitude is 3 dB lower than the peak, ending at the other -3 dB frequency which higher than this nature frequency..

## 2.4 Radiation

The previous sections reveal the bending waves behaviours on plates and the modal approach, all of which concern about the vibration of the plate; however, radiation is the least thing one can skip while having discussion about loudspeakers. Without the interactions between vibrating panel and air, one will never hear sounds. Therefore, it

is imperative to understand the nature of sound radiation and the approaches which different types of loudspeakers apply.

### 2.4.1 Monopole

Monopole usually represents an omni-directional sound source. It is called as point source if the dimension of the sound source is relatively small in comparison with the wavelength, which is usually the case for low frequencies. It is significant elementary sound source because most of complicated sound source can be considered as the combination of many monopoles, thus the response of the sound source is able to be thought as the summation of individual monopoles. The derivation of the solution of monopole to wave equation, Eq (2.30), is beyond the scope of this thesis. One who is interested in the derivation process can look up Chapter 6 of [4].

$$\Delta p + k^2 p = 0 \quad (2.30)$$

, where  $p$  represents the pressure and  $k$  is the wave number.

Thus the solution is given:

$$p(r) = v_a \frac{a^2}{1 + jka} \frac{1}{r} e^{-jk(r-a)} \quad (2.31)$$

where  $a$  the radius of the monopole,  $r$  the distance from the centre of the sound source to the observation position,  $v_a$  the sound velocity at the boundary of the monopole, i.e.  $r=a$ .  $v_a$  is defined as:

$$v_a = \frac{A(1 + jka)e^{-jka}}{j\omega\rho a^2} \quad (2.32)$$

$A$  is a constant which represents the amplitude of the source.

By using the relationship between the sound velocity and the pressure, namely Eq (2.33), one can calculate the velocity as a function of  $r$  as Eq (2.34):

$$v = -\frac{1}{j\omega\rho_0} \frac{\partial p}{\partial r} \quad (2.33)$$

$$v(r) = v_a \frac{a^2}{1 + jka} \frac{1 + jkr}{r^2} e^{-jk(r-a)} \quad (2.34)$$

One might include the effect of time by multiplying Eq (2.31) and Eq (2.34) with  $e^{j\omega t}$ .

$I$ , the intensity, is therefore available by using the pressure and the sound velocity, and so is the sound power  $W$ , which is shown in Eq (2.35).

$$W = \int_s I ds = \int_s \frac{1}{2} \text{Re}\{p \cdot v^*\} = 2\pi a^2 v_a^2 \rho c \frac{k^2 a^2}{1 + k^2 a^2} \quad (2.35)$$

where  $\rho$  the air density,  $c$  the sound speed in air.

Eq (2.35) can be further simplified respectively for low and high frequencies, i.e.  $ka \ll 1$  and  $ka \gg 1$ .

At low frequencies:

$$W \approx 2\pi a^2 v_a^2 \rho c k^2 a^2 \quad (2.36)$$

As for high frequencies:

$$W \approx 2\pi a^2 v_a^2 \rho c \quad (2.37)$$

One can see that at high frequencies the sound power is frequency-independent. Therefore the radiated power is nearly constant at high frequencies while it is proportional to the square of wave number  $k$ , i.e. increasing with the square of frequency  $\omega$  at low frequencies.

In practical, one can approximate most of common electro-dynamic loudspeakers by means of a monopole at low frequencies, but the high frequency approximation is rarely applied. The first reason is that most of the diaphragms of the loudspeakers are better approximated to perfect piston at low frequencies instead of high frequencies. The other reason is that the imaginary part of the impedance becomes significant at high frequencies therefore affect the motion of the diaphragm.

## 2.4.2 Infinite plate radiation

A plate with infinite size is another basic radiator which helps the analysis of a complicated sound source. Most of the bending wave loudspeakers which will be introduced in next chapter apply such approach, therefore the detailed explanation and physical phenomena need to be exhibited here.

Consider a plate as sketched as Figure 2.4 which extend to infinity at both side, meaning no reflections is going to come back to interfere the sound field.

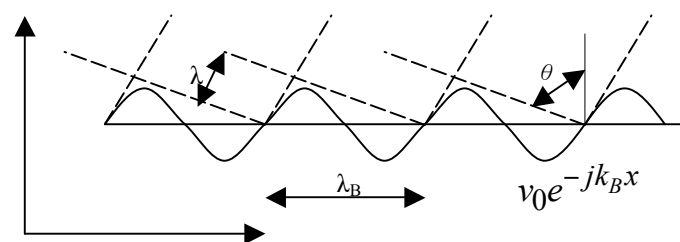


**Figure 2.4 Sketch of Infinite Plate**

The velocity is a function of the wave number  $k_B$ :

$$v(x) = v_0 e^{-jk_B x} \quad (2.38)$$

And the pressure  $p$  can be assumed in this form:

$$p(x, y) = p_0 e^{-jk_B x} e^{-jk_y y} \quad (2.39)$$

This expression of pressure should satisfy the wave equation, cf. Eq (2.30), yielding that

$$p_0(k^2 - k_y^2 - k_B^2)e^{-jk_Bx}e^{-jk_yy} = 0$$

which is valid only if:

$$k_y^2 = k^2 - k_B^2 \quad (2.40)$$

Once again, by using the relationship of velocity and pressure, i.e. inserting Eq (2.39) into Eq (2.33), one may have:

$$v_0 = v|_{x=0,y=0} = \frac{p_0 k_y}{\omega \rho}$$

From which one finds that

$$p_0 = \frac{v_0 \omega \rho}{k_y} = \frac{v_0 \rho c k}{k_y} \quad (2.41)$$

Combine Eq (2.39), (2.40), (2.41), it yields a general equation of pressure for infinite plate

$$p(x, y) = \frac{v_0 \rho c k}{\sqrt{1 - k_B^2/k^2}} e^{-jk_Bx} e^{-j\sqrt{k^2 - k_B^2}y} \quad (2.42)$$

And the velocity is

$$v(x, y) = v_0 e^{-jk_Bx} e^{-j\sqrt{k^2 - k_B^2}y} \quad (2.43)$$

Observing Figure 2.4, one may have the radiated angle  $\theta$  in terms of the wave length, which implies it can also be presented in wave number, i.e.

$$\sin \theta = \frac{\lambda}{\lambda_B} = \frac{k_B}{k} \quad (2.44)$$

For bending waves, recall Eq (2.15), the radiated angle is:

$$\theta = \sin^{-1} \frac{\lambda}{\lambda_B} = \sin^{-1} \frac{c}{c_B} = \sin^{-1} \left( \frac{c}{\sqrt{\omega}} \sqrt[4]{\frac{m''}{B}} \right) \quad (2.45)$$

From which one can see that higher the frequency, smaller the radiated angle.

It is noted that in Eq (2.42), the pressure will be imaginary unless  $k_B \leq k$ , that is  $c_B \geq c$ , indicating no radiation occur below certain frequency and the frequency where the pressure becomes real is often of interest. At this frequency, the wave speed of the plate vibration is identical to the ambient media, air here, and radiation starts to occur. This particular frequency is called coincident frequency or critical frequency  $f_c$ . As for bending waves, it can be calculated as:

$$f_c = \frac{c^2}{2\pi} \sqrt{\frac{m'}{B}} \quad (2.46)$$

Consequently, the critical frequency split the frequency range into two parts: below  $f_c$  and above  $f_c$ . Above  $f_c$ , sometimes called far field, the pressure in Eq (2.42) can be in terms of radiated angle, yielding

$$p(x, y) = \frac{v_0 \rho c}{\cos \theta} e^{-jk_B x} e^{-jk_y \cos \theta} \quad \text{for } \lambda_B > \lambda \quad (2.47)$$

The relation between the radiated power and the structure vibrations is generally desired, which is usually described in terms of the so-called radiation efficiency. The radiation efficiency  $\sigma$  is defined as the ratio between the radiated sound power of the sound source  $W$  and the radiated sound power of a plane radiator,  $W_{\text{plane}}$ , both of which are with the same averaged root-mean-square velocity  $\tilde{v}$  all over the surface  $S$ . In formula, it is

$$\sigma = \frac{W}{\rho c S \tilde{v}^2} \quad (2.48)$$

In this case, it is

$$\sigma = \frac{1}{\cos \theta} = \frac{k}{\sqrt{k^2 - k_B^2}} \quad \text{for } \lambda_B > \lambda \quad (2.49)$$

Below  $f_c$ , the wavelength of the sound in the ambient medium is larger than the wavelength of the vibration of the plate, denoting that the radiation does not occur.

In this case, Eq (2.42) becomes:

$$p(x, y) = \frac{jv_0 \rho c}{\sqrt{\frac{k_B^2}{k^2} - 1}} e^{-jk_B x} e^{-\sqrt{k_B^2 - k_y^2} y} \quad \text{for } \lambda_B < \lambda \quad (2.50)$$

The velocity in x and y directions the may be found from Eq (2.43)

$$\begin{cases} v_x = \frac{jk_B v_0}{\sqrt{k_B^2 - k^2}} e^{-jk_B x} e^{-\sqrt{k_B^2 - k_y^2} y} \\ v_y = v_0 e^{-jk_B x} e^{-\sqrt{k_B^2 - k_y^2} y} \end{cases} \quad (2.51)$$

and from Eq (2.50) and Eq (2.51) one can see the sound pressure and the plate velocity are 90 degree out of phase, and no sound is radiated. Therefore, the radiation efficiency is 0 when the frequency is below  $f_c$ .

At the coincidence frequency, the case has not be shown yet, one can see the pressure will become infinite from Eq (2.42) and the radiation angle will be 90, as one can infer from Eq (2.45). The radiation efficiency will then be infinite, too. Nevertheless, this is not going to happen in practice because first of all, no infinite plate does exist, and secondly, the loading of the radiating surface under this condition is very high, resulting in limit vibration on the surface, leading to limit sound pressure.

The motion of the air particles near the plate are often of interests. In near field, that is below  $f_c$ , they are actually moving around as ellipses [4], as sketched in Figure 2.5, instead of moving forward and back, which is the case for far field. The elliptical motions can be interpreted as the particles moves laterally to escape from compression, which is necessary to generate a sound wave. Thus it can be regarded as

hydrodynamic short circuit if one uses an analogues circuit to describe the acoustic system.

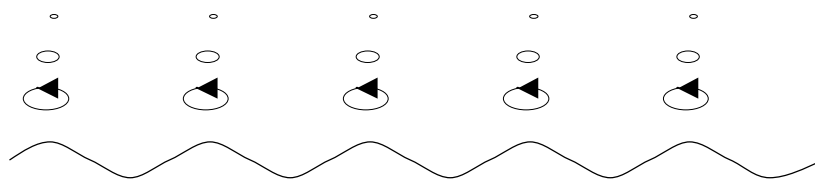


**Figure 2.5 Particle motions in near field radiation**

However, for the loudspeaker of finite plate which apply infinite plate approach, the radiations do not occur is not exactly true. One needs to consider that a near field at the excitation point will be excited and the leakage might occur as shown in the next subsection.

### 2.4.3 Finite plate

A common way to describe the vibration pattern of a finite plate is to assume an infinite plate is covered by an infinite baffle with an aperture whose size is identical to the size of the finite plate. Therefore, the velocity of the finite plate  $v'$  can be expressed in terms of the velocity of the infinite plate  $v$  and an aperture function  $a$ :

$$v'(x, y) = v(x, y) \cdot a(x, y) \quad (2.52)$$

$$\text{Where } a(x, y) = \begin{cases} 1, & \text{if } (x, y) \text{ is inside the aperture} \\ 0, & \text{if } (x, y) \text{ is outside the aperture} \end{cases} \quad (2.53)$$

The wave spectrum of vibration  $V'(k_x, k_y)$ , the spatial Fourier transform of  $v'(x, y)$ , is then

$$V'(k_x, k_y) = V(k_x, k_y) * A(k_x, k_y) \quad (2.54)$$

where “\*” denotes convolution. One can notice  $V(k_x, k_y)$  should be imaginary below critical frequency, that is when  $k_B$ , i.e.  $k_x^2 + k_y^2$ , is bigger than  $k^2$ , since  $v(x, y)$  is imaginary below  $f_c$ . Therefore the convolution sign implies the aperture effect will results in leakages below the critical frequency  $f_c$  for  $V'(k_x, k_y)$ . Because of that, the finite plate can have nonzero radiation below  $f_c$ .

With the knowledge of wave number spectrum, one might calculate the sound pressure by the use of the following equation, which is the consequence of applying Rayleigh integral on a finite plate mounted in rigid baffle:

$$p(R, \omega) = \frac{j\omega\rho}{2\pi} \frac{e^{-jk_0R}}{R} V'(k_x, k_y) \quad (2.55)$$

, where  $R$  is the distance from the centre of the plate to the observation position.

As for radiated power, it is given by

$$W_{rad} = \frac{\rho c}{8\pi^2} \iint_{-k}^{+k} \frac{k |V'(k_x, k_y)|^2}{\sqrt{k^2 - k_x^2 - k_y^2}} dk_x dk_y \quad (2.56)$$

One may use the relation between the wave spectrum  $V'(k_x, k_y)$  and the exciting pressure distribution  $P(x, y)$ , and the relation between the exciting pressure distribution  $P(x, y)$  and the exciting point force  $F$  to rewrite Eq (2.56), along with the expression  $k_x = k_r \sin \varphi$  and  $k_y = k_r \cos \varphi$ .

$$W_{rad} = \frac{\rho c \omega^2 \hat{F}^2}{4\pi^2 B'^2} \int_0^k \frac{k k_r}{[k_r^4 - k_B^4] \sqrt{k^2 - k_r^2}} dk_r \quad (2.57)$$

Again, one may discuss the radiated power by distinguishing above and below critical frequency  $f_c$ .

As for below  $f_c$ , Eq (2.57) can be simplified by using the approximation of  $k_B^8 \approx [k_r^4 - k_B^4]^2$

Therefore,

$$W_{rad} \approx \frac{\rho c \tilde{F}^2 k^2}{2\pi \omega^2 m''^2} = \frac{\rho \tilde{F}^2}{2\pi c m''^2} \quad \text{for } f \ll f_c \quad (2.58)$$

It is obvious that the radiated sound power is frequency-independent, but only dependent upon the excitation force and the mass per unit area of the plate. In other words, the sound power is constant, as the frequency is much lower than the critical frequency. Another surprising thing is that the radiated power is independent of flexural stiffness  $B$ . If one applies the constant point impedance  $Z_0$ , namely  $Z_0 = 8\sqrt{Bm''}$ , Eq (2.57) can be expressed in terms of critical frequency.

$$W_{rad} = \frac{8}{\pi^3} \rho c v_0^2 \lambda_c^2 \quad (2.59)$$

, where  $\lambda_c$  the wavelength at critical frequency,  $v_0$  the velocity at the excitation point.

Eq (2.59) reveals the fact that for a fixed value of  $v_0$ , the radiated power decrease as the wavelength at critical frequency decrease, i.e. the critical frequency increase. This also implies the bending stiffness decrease if the mass per unit area remains the same, ref. Eq (2.46).

With sound power, it is then intuitive to investigate the efficiency. Therefore, one needs to divide Eq (2.58) by the following Eq (2.60), which expresses the mechanical input power.

$$W_{in} = \frac{1}{2} |v_0|^2 \text{Re}\{Z_0\} \quad (2.60)$$

The efficiency  $\eta$  is then

$$\eta = \frac{2\rho\lambda_c}{\pi^2 m''} \approx \frac{1}{5} \frac{\rho\lambda_c}{m''} \quad (2.61)$$

It is seen that the efficiency can be approximated by the ratio of the mass of a one-fifth wavelength thick layer of the ambient medium to the mass of the plate. In practice, the efficiency is usually low.



### 3 Design of Bending Wave Loudspeakers

Four different kinds of designs of commercial bending wave loudspeakers are exhibited here, including the bending wave loudspeaker from Göbel, the DDD driver of German Physiks, the bending wave sound transducer from Manger, and the last but the most important Distributed Mode Loudspeaker, short as DML, from NXT. DML is important not only because it is a new technology which means it has many possibility to be dig out, but also because it is the sample which will be used for the measurement in the next chapter.

#### 3.1 The Bending Wave Loudspeaker of Göbel

Göbel produces a bending wave loudspeaker based on the infinite panel approach. See Figure 3.1 for illustration.



Figure 3.1 The Bending Wave Loudspeaker of Göbel Corp. [5]

The edge of the panel is well cut by lasers in order to reduce the reflection from the boundaries thus achieve the infinite panel approach. Besides, it also can be use for adjusting the moment of inertia  $I$ , or the bending stiffness  $B$ . The panel of this bending wave loudspeaker consists of 9 layers, which is mainly made of a special tropic wood, with a remarkable property of anisotropy. The in-homogeneity of the wood avoids distinctive resonance occurring on the panel. It is claimed that “the particular mass density and damping characteristic of the panel also enables the panel to radiate well even below the critical frequency”; however, it is not surprising. As one remember, it is already pointed out in Sec 2.4.2 that for any plate apply infinite approach, there will be some leakage occurring below critical frequency. The question left is that how well is the frequency response below  $f_c$ . Is it flat enough? How is the efficiency at LF? It is a pity that no information about these details is given from their website. One who is curious may try to contact with them. More for the panel, the clamping consists of sophisticated damping made of rubber, aluminium, silicon, foam rubber and so on, to have a well-controlled frequency limit.

Strictly speaking, the design principle of this bending wave loudspeaker is nothing more than an infinite panel approach. The distinctive thing of the loudspeaker is the art of producing, including the clamping, manufacture of the panel and especially the material selection. If the resonant frequencies really can be eliminated by using this 9-layers design, then one can expect that the sounds it reproduced should be very clear.

Unfortunately the sample of this loudspeaker is not retrieved that no further test can be done. A commenting article about this loudspeaker [6] is found and the author seems very satisfied with its crystal sound and isochoric dispersion properties. The author also mentioned that due to its nature properties of dipole directivity, the room is flooded with music thus even one leaves the sweet spot the music still sounds wonderful. It hints the common and famous merit of BWL and DML: a diffuse sound field, which will be testified in the next chapter for DML.

### 3.2 The DDD driver of German Physiks

At the first glance on the DDD driver of German Physiks, see Figure 3.2, it might look like a conventional piston-like driver, which is in the shape of cone, with magnet equipped actuator at the bottom of the cone. But it works very different from piston driver.

Let's begin with the mounting and the motion of the actuators. While playing sounds, the actuator of the conventional driver usually move along the axis of the cone, as well as the diaphragm. Thus sounds will be radiated in the direction of the actuator's motion; on the other hand, the mouth of the DDD driver is usually mounted on the chassis, which is often the box of the subwoofer. Therefore when DDD driver is in action, the diaphragm does not move with the actuator, but start to bend over, creating bending waves on the diaphragm (the cone) and commence to radiate from it. See Figure 3.3 (a) and (b) for illustration.



Figure 3.2 The Dicks Dipole Driver, or DDD, driver. [1]

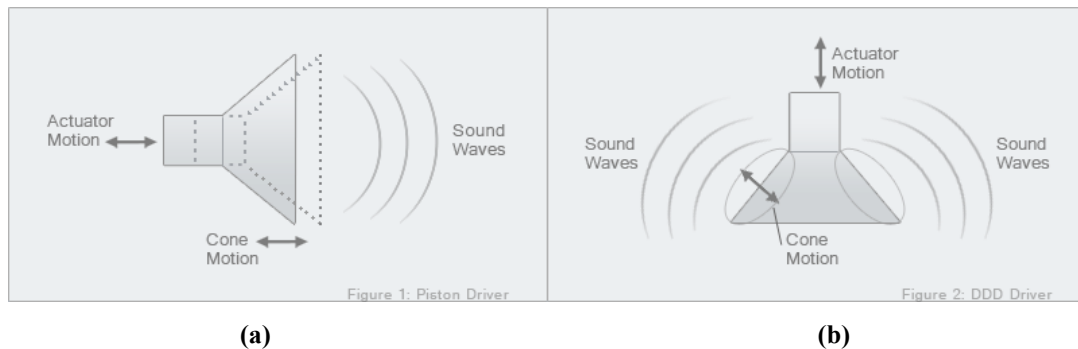


**Figure 3.3 The illustrations of the action of (a) conventional piston driver and (b) DDD driver. [1]**

As claimed by German Physiks, the DDD driver works great differently for four frequency bands:

The upper limit of lowest frequency band can be explained by Small/Thiele resonant parameters; in the second frequency band up to the first coincidence frequency, it works as a piston driver. The “first” coincident frequency is emphasized here because that is due to the shape of the diaphragm and the dispersion nature of bending waves, thus the critical frequencies are spread over the entire cone; the third frequency band is a transition band. The piston like radiation is gradually replaced by bending wave radiation. This band is up to the last coincidence frequency of driver; in the last frequency band, it works as a pure bending wave loudspeaker.

The cone’s stiffness is decreased from the throat (the bottom side of the actuator) to the mouth, therefore the speed of the bending waves also decreases while travelling forward to the mouth, ref. Eq (2.14), resulting in that the bending waves becomes more easily to meet the coincident frequency in the progress of transmitting, even for higher frequencies. By using this implementation, the radiation efficiency is increased thus the waves reflected by the mounted boundary of the mouth is consequently well weakened, thus the resonances of the cone can be greatly reduced. Since the DDD driver is responsible for all frequencies except the bass, usually subwoofers are equipped with their loudspeakers. Like typical electromagnetic loudspeakers, the DDD driver is also mounted on an enclosure to make the rear waves available, as depicted in Figure 3.4.



**Figure 3.4  
A typical design  
of German  
Physiks's  
loudspeakers  
which employs  
two DDD  
drivers. (Type  
PQS 402) [1]**

If one ponders about this design of DDD driver, one will comprehend that the design of it is actually based on the infinite plate approach, too. However, instead of a

flat panel, a cone-shape is used to achieve the more omni-directional directivities, which is in fact a distinctive merit emphasized by German Physiks, that the DDD driver behaves nearly a point source. Nevertheless, a varied stiffness of the excited structure is a clever idea, which not only increases the radiation efficiencies but also avoid the resonance occurring at certain frequencies, causing unwanted resonant sounds. But another question comes up at the same time. No matter how the stiffness is alternated, it always concerns the change of the density or the thickness of the cone. Either way leads to the change of the impedance and one knows that the waves will be reflected when the impedance along waves' travelling is not consistent. Even though the difference of impedance of adjacent positions is small, it still could cause reflections and hence excite modes. The question is if the reflections can be reduced to very weak compared to the incident waves; nevertheless, this will not be further studied here since this loudspeaker is too expensive to purchase as a test sample.

The trick of this design is to merge the ideas and the advantages of the electro-dynamic loudspeakers and the panel bending wave loudspeaker, making it a splendid product. This smart design and its resultant difficulties of producing are also reflected by its extremely high price, which is exactly the reason make the sample of this type of loudspeaker not possible to be acquired, thus it is only simply introduced and commented here.

### 3.3 The Sound Transducer of Manger

Like the previous two cases, the sound transducer from Manger also applies the infinite plate approach. In addition, a solution similar with the DDD driver for dispersive nature of bending wave is employed, that is to utilize a changing stiffness for the diaphragm. The difference between these two plans is that Manger uses a rigidity increasing from excitation position (the centre) to the edges of the diaphragm, which makes the high frequencies reach the coincident frequencies immediately after being excited, making the waves start to be radiated without long travel. In contrast with that, the rest, namely lower frequencies gradually speed up and eventually meet the sound speed of air while travelling to the boundaries. Figure 3.5 illustrates this phenomenon [2].

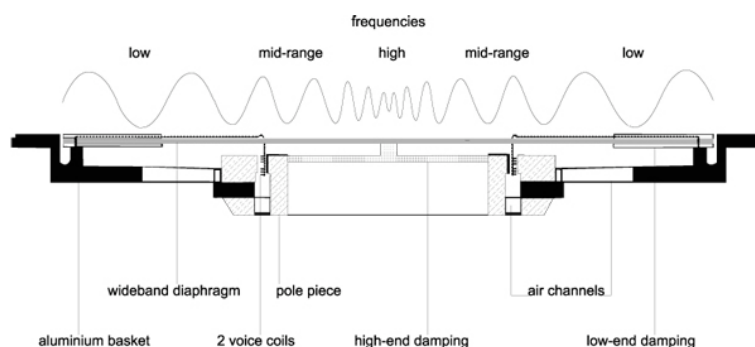


**Figure 3.5 Illustration for bending waves' travelling and radiation and the compositions of the transducer [2].**

The low frequencies are absorbed by the star-shaped dampers at the edges of the membrane, leading to few reflections caused by the boundaries. Hence the infinite plate approach is accomplished. Another characteristic design of it is that it applies two voice coils mounted mechanically in series and switched electrically in parallel, in order to fulfil the requirements of reproducing the bass band at the same time, i.e.

larger displacement and instant movement. This makes the coil long enough to handle for low frequencies but remains a very light mass.

The beauty of infinite panel approach, the constant pure real driving point impedance, is stressed by Manger. It is reported that because of this property, the velocity of the panel can follow the force very well, leading no transition errors like the common electro-dynamic loudspeakers do. As matter as fact, the other loudspeakers using infinite plate approach should have the same merits, meaning the loudspeakers introduced in previous two sections should also have little transition errors.

Same as the previous types of bending wave loudspeaker, the sample of Manger's transducer is not available, but the theory of it is examined by the famous scientist in physical acoustic, Dr. Manfred Heckl, ref. [2]. It is said that the principle applied by Manger yields the radiation history corresponding to the current history, namely no transient oscillations occur.

## 3.4 The Distributed Mode Loudspeaker of NXT

### 3.4.1 Introduction

The Distributed Mode Loudspeaker, abbreviated as DML in the following sections, is the last but the most significant one here. It is important not only because it is a new technology which implies that it has many possibilities to be unearthed, but also mainly due to that it is the sample which will be tested for the next chapter. The discovery of the possibility of DML is a beautiful accident. It is found during a trail to improve the sound isolation but somehow found that the availability of a panel for radiation due to the resonances.

It is stated in Section 2.3 that a panel might have infinite modes, and the velocity and the radiation of the panel can be represented by the summation of the contribution of modes. Since this kind of speaker employs resonances of the panel, or modes, respondent for radiation, and the modes are distributed all over the panel, thus it is named as the "Distributed Mode Loudspeaker".

### 3.4.2 Acoustic analogous circuit

The construction of a DML can be quite simply, which may only consists of an exciter and a panel which the exciter is attached to. A simplified model of DML using a moving-coil can be drawn as Figure 3.5, which mechanically behaves like a spring-mass system, in which the plate is assumed to be vibrating randomly. In addition, the energy given to the plate is presumed to be fully radiated, meaning no mechanical loss is considered since in reality it is very low in comparison with dissipation.

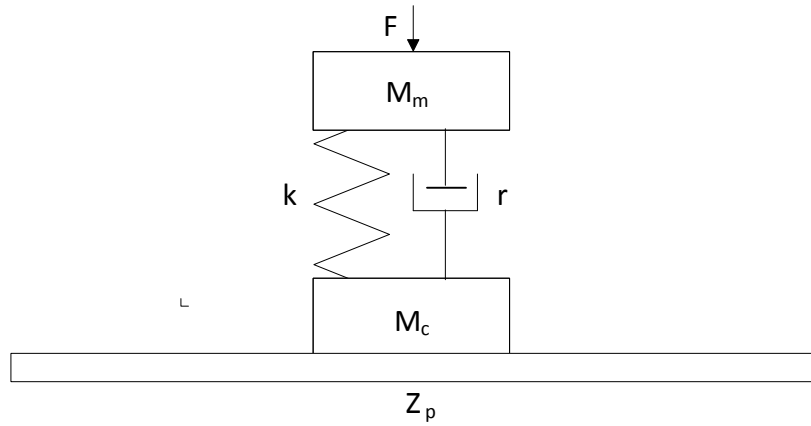


Figure 3.5 The DML as a mass-spring system, where  $F$  the applied force,  $M_m$  the mass of the magnet,  $M_c$  the mass of the coil,  $Z_p$  the impedance of the panel,  $r$  damping of the attachment,  $k$  the spring constant of the attachment

Figure 3.6 shows an analogous circuit of impedance which is often applied for analyzing DML system shown in Figure 3.5.

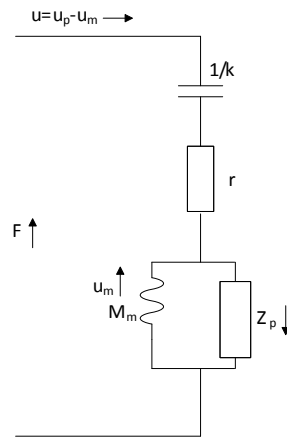


Figure 3.6 The analogous circuit of mechanical impedance, where  $u$  the velocity of the spring and damper,  $u_m$  the velocity of the magnet,  $u_p$  the velocity of the plate.

The effective impedance in Figure 3.6 is then:

$$Z_{m_{eff}} = Z_p' \left( 1 - \frac{k}{\omega^2 M_m} \right) + r + \frac{j}{\omega} \left( k + \frac{r Z_p'}{M_m} \right) \quad (3.1)$$

Where  $Z_p' = R_p + jX_p + j\omega M_c$

At high frequencies, Eq (3.1) can be simplified as:

$$Z_{m_{eff}} \approx Z_p' + r = (R_p + r) + j(X_p + \omega M_c) \quad (3.2)$$

Since  $R_p$  and  $\omega M_c$  dominate Eq (3.2), it can be further simplified, the effective impedance becomes:

$$Z_{m_{eff}} \approx R_p + j\omega M_c \quad (3.3)$$

One wants the effective impedance of DML is purely resistive, implying that the imaginary part in Eq (3.3) has to be much smaller than the real part. This gives the approximate upper frequency limit of DML:

$$f_{upper} \approx \frac{R_p}{2\pi M_c} \quad (3.4)$$

By the same token, the lower limit frequency can be found by using low frequency simplification, where  $k$  is presumed to be ignorable.

$$f_{lower} \approx \frac{R_p}{2\pi M_m} \quad (3.5)$$

One may have the electrical impedance by using the force factor  $Bl$  to convert the impedances between the mechanical part and the electrical part. Therefore, the electrical impedance  $Z_e$  is given:

$$Z_e = Z_{coil} + \frac{Bl^2}{Z_{m,eff}} \quad (3.6)$$

where  $Z_{coil}$  is the impedance of the coil.

In addition,  $Z_p$  the point impedance of the plate is often approximated by using the point impedance of a thin and isotropic infinite plate, derived by Cremer et al [4], as shown in Eq (3.7).

$$Z_p = 8\sqrt{Bm''} \quad (3.7)$$

where  $B$  the bending stiffness,  $m''$  the mass per unit area.

### 3.4.3 Frequency response and polar response

As mentioned in Section 2.3, the spatial velocity distribution of the panel can be solved if the geometry of the object and the boundary conditions are simply. If not, it still can be solved by software applying finite elements methods, such as Comsol Mutiphysics. With the knowledge of the spatial velocity distribution, the sound pressure can be foretold if one applies the Raleigh's integral. It is reported that the modelled result gives rational agreements with the measurement in [8].

Because of bending waves' properties, the coincident angles vary for different frequencies and the coincidences happen all over the vibrating panel, resulting in that the sounds radiated by DML are very diffusive and bi-polar. On the other hand, the conventional speakers suffer from well-known beaming problem at high frequencies.

The radiation of DML can be well modelled by considering DML as an infinite panel behind an aperture cut into infinite baffle, as per [9]. Bank used a commercial solver to simulate the polar response of DML, showing that the polar response is actually independent of the size of the plate, except bass band, but varies on where coincidences occur [10]. At the critical frequencies, DML will exhibit a little beaming behaviour, too [11].

### 3.4.4 Sound power

It is known that the sound power of a randomly vibrating panel is proportional to the spatial and time averaged square velocity  $\hat{v}^2$ , and the spatial and time averaged square velocity  $\hat{v}^2$  is also proportional to the driving point velocity. Since the impedance is resistive, the driving point velocity for a given force will be nearly constant. Consequently, the sound power will be approximately constant, as already shown in Sec 2.4.3.

However, in the case of electro-magnetic loudspeaker, the acceleration of the diaphragm is constant for a given force (Newton's second law) since it is designed to vibrate as a rigid body, inferring that the velocity is inverse proportional to frequency. The radiation resistance is introduced by Bernek in 1996 that it is nearly constant for high frequency. Thus the radiated sound power for electro-dynamic loudspeaker is then:

$$W_R = \frac{1}{2} R_R |v_c|^2 \sim \omega^{-2} \quad (3.8)$$

which indicates that the sound power level will descend 6 dB / octave band.

As for low frequency ( $ka < 1$ , where  $k$  the wave number,  $a$  the radius of the diaphragm), it can be approximated as a monopole, which means it can be represented by Eq 2.36. As one can observe, the radiated sound power increase with the square of frequency, i.e. ascend 6 dB/ octave band.

### 3.4.5 Excitation point, material of panels, and geometry of panel

As already emphasized so many times, DML works by the principle of modes; therefore the optimization of modes' distribution is a significant issue. It is dominated by the shape and the size of the panel, the material's properties (mainly the stiffness and the density), and the excitation point.

The position of the exciter will decide which modes of the plate will be excited, affecting the radiation performance of DML. Thus it is essential that one makes sure that the excitation point couples as many modes as possible, and ensures de-correlation between panel velocity and drive point. One might use, again, FEA to determinate the position of the exciter. Usually observing the first 20 modes or so is sufficient to conclude the optimal point of exciter, which is often near the middle point of the panel but never exactly on it. This is because that while the exciter is on the middle, it only can excite even modes. Figure 3.5 illustrates the nodal maps of the first 20 modes of a panel quoted from [9], which can be done by using FEM. The region where fewer nodal lines pass is a better position for exciter; in this case, possible choices are near the middle and the corners.

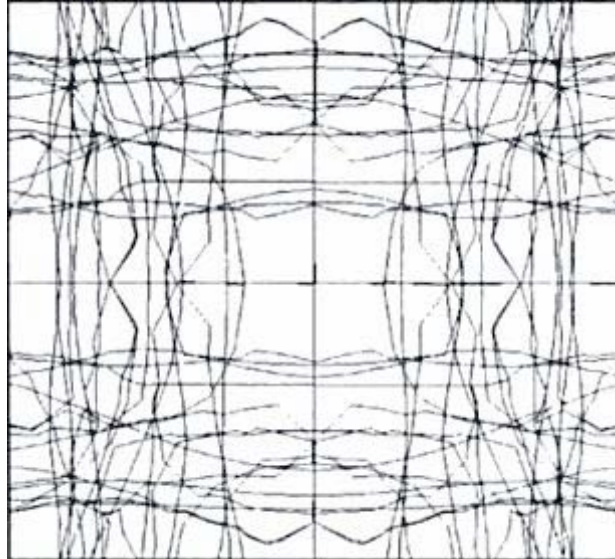


Figure 3.5 The illustration of the first 20 modes of a DML panel [9].

Panel geometry decides modes frequencies. As for DML, it is common to apply rectangular as the shape of the panel, therefore the ratio of the length to width becomes a vital parameter which controls the performance of the modes, as per Eq (2.23). A simulation for finding the optimal ratio of length to width to achieve the most even distribution of modes will be presented in Chapter 5. In addition, another optimization method called genetic algorithm, which will not be used in this thesis due to the unavailability, is confirmed that it could optimize the modes distribution by trading between the excitation position and the surface ratio [18] [19].

Besides, the construction of the panel also matters, since it determines the moment of inertia  $I$ , influencing the bending stiffness  $B$ . Typically speaking, one prefers complex structure such as honeycomb or multi-layer structure to isotropic structure because they give more possibilities to achieve certain bending stiffness  $B$ , in order to implement a specific ratio of  $B$  to  $m''$ , the mass per unit area.

The material of the panel is also dominant in Eq (2.23) because the mass per unit area  $m''$  also influences the ratio of  $B$  to  $m''$ . Usually one wants the fundamental frequency  $f_0$ , i.e. the first nature frequency, as low as possible such that the low frequency can be well covered since the feasible lower frequency limit is set to be  $2.5 f_0$  as per [10]. The first nature frequency can be obtained by using Eq (2.23) or the following approximation:

$$f_0 \approx \frac{\pi}{A} \sqrt{\frac{B}{m''}} \quad (3.9)$$

where  $A$  the surface area.

As a consequence, one usually wants the  $B/m''$  ratio lower, which means either the mass per unit area should be higher, or the bending stiffness should be lower. The choice is often to find a material with lower bending stiffness since high density implies low radiated sound power and that is usually one does not want to see.

Another important reason to keep  $f_0$  low is that the asymptotic modal density is inversely proportional to the ratio of bending stiffness  $B$  and the mass per unit area  $m''$ , and one wants it as high as possible. The same reason applies for the critical frequency, because below the critical frequency the directivities of DML behave more

omni-directional. However, to achieve a proper radiation efficiency and radiated sound power, the Young's modulus cannot be too low. Thus one needs to carefully trade between  $E$  and the density  $\rho$  to accomplish one's goal of designing.

## 4 Performance of loudspeakers

### 4.1 Introduction to the test samples

Two types of loudspeaker are under study here. The first one is a sample of Distributed Mode Loudspeaker from NXT. The panel of it has the dimensions of 20 cm long, 17 cm wide and 1.2 mm thick. The panel is constructed by light and semi-transparent material and made in the form of honeycomb, with unknown density and Young's modulus. The exciter of this radiator has the diameter of 4.5 cm, mounted at the position of 7.2 cm from a corner on the shorter side of the panel and 8.6 cm away from this corner on the longer side. See Figure 4.1(a) and (b) for details.

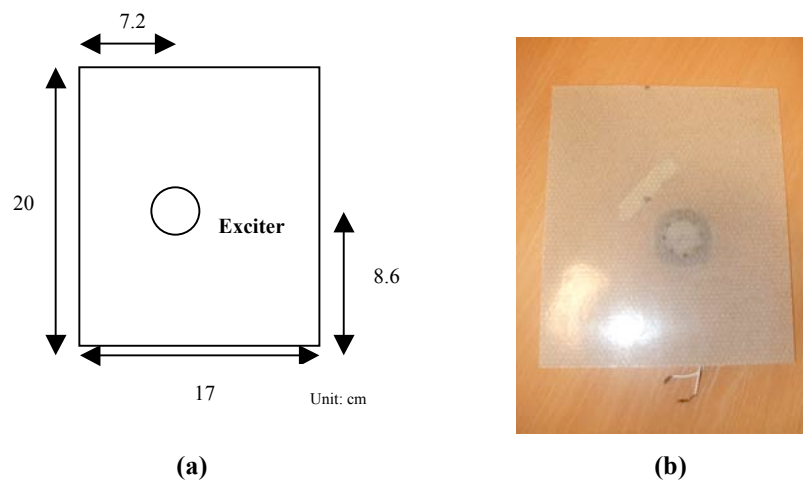


**Figure 4.1**(a)The geometry of the DML and the position of the exciter  
(b) The photo of the sample DML

The other loudspeaker is a conventional electro-dynamic multimedia loudspeaker with a box, designed and produced by Apple Computer Inc. The purpose to introduce this speaker here is to use the most common type of loudspeaker as a reference that DML can be compared with. The speaker has a radiator with radius of 3.7 cm roughly located in the middle of the box. The mounted box is 19 cm high, 6.7 cm wide and 9.05 cm long. See Figure 4.2 for details.

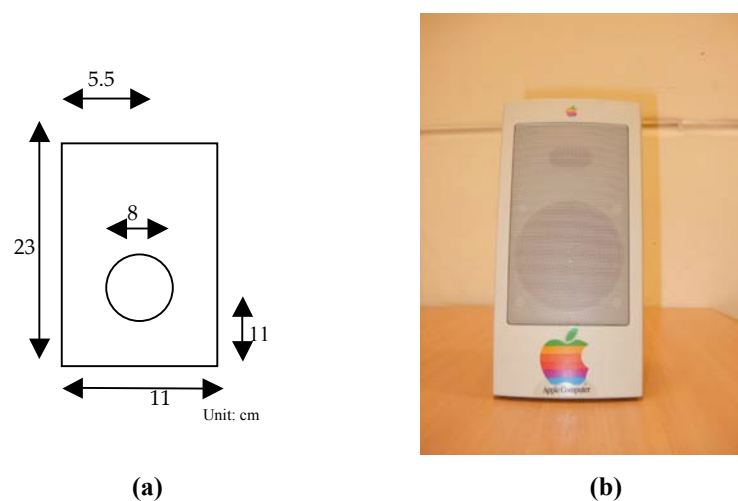


**Figure 4.2**(a) The geometry of the conventional multimedia loudspeaker (b) the photo

The two loudspeakers will undergo a series of measurements, including the measurement of impulse response – also implying frequency response –, directivities, sensitivities, distortions, efficiencies, sound power, and the SPLs distribution in a low reverberant room. The impedance of the panel of the DML will be also measured to understand the mechanical properties of the panel. In these measurements, the DML had been fixed on two rods by tapes in order to minimize the effect of the boundary condition and also to achieve a common way of clamping while using DML; that is, hanging near the wall.

## 4.2 Material properties

Since the material properties of the given sample of DML are unknown, it is intuitional to measure these characteristics for the very first measurement. However, these mechanical testes need a strip of the panel as the test sample and cutting a piece from the DML will definitely change the properties permanently, no matter mechanically or acoustically. Therefore, it is actually the last experiment performed on the DML. An excitation test is carried out to find out the Young' modulus and the loss factor of the plate by the use of Complex Modulus Apparatus Type 3940, as illustrated in Figure 4.3. Two small pieces of irons are attached to the strip on positions close to the locations of pick-up and the exciter. Consequently, while the exciter is in operation, it generates a magnetic field that the iron piece near the exciter on the strip is magnified. Thus it will move accordingly with the exciter's input therefore drive the whole strip. Consequently, the information of displacement can be given by the movement of iron piece near the pick-up. Finally the resonance is received at the pick-up. See Figure 4.4 for the set-up.

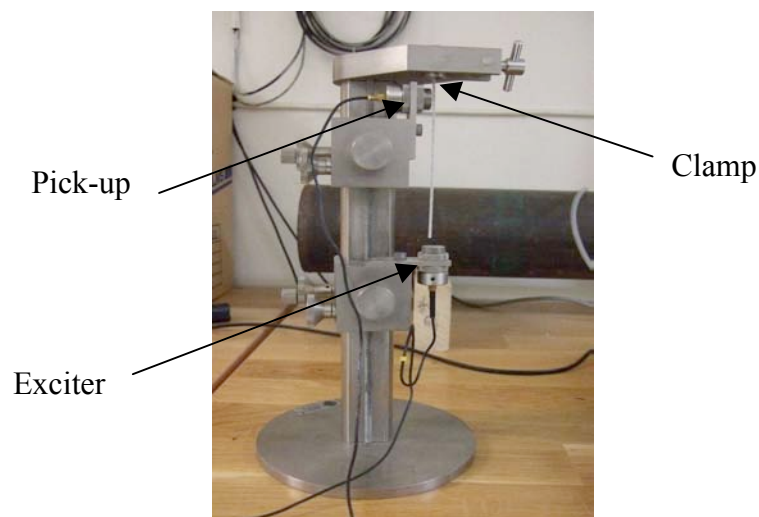


**Figure 4.3** The photo and parts' illustration of Complex Modulus Apparatus Type 3940.

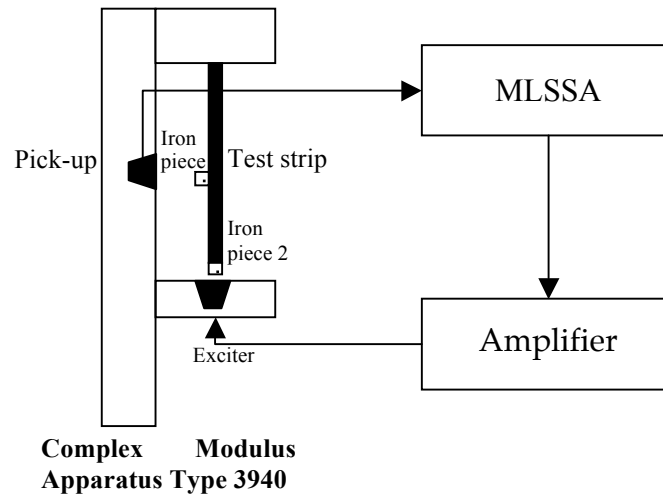


**Figure 4.4 The set-up of Young's modulus and loss factor.**

By means of the set-up illustrated in Figure 4.4, one could follow the instructions given in the manual of Complex Modulus Apparatus Type 3940 to acquire the impulse response. Thus frequency response could be acquired simply by applying FFT to impulse response, as drawn in Figure 4.5. The peak at around 50 Hz is recognized as the second mode and the one at 150 Hz is regarded as the third mode. It might be questioned why the one at 50 Hz is not the first mode. That is because there are certain ratios between the first some nature frequencies, suggested by the manual: the second resonant frequency should be around 6 times of the first one and the third one must be around 3 times of the second one. Therefore the assumption of 50 Hz as the 2<sup>nd</sup> and 150 Hz as the 3<sup>rd</sup> fits the suggestion better.

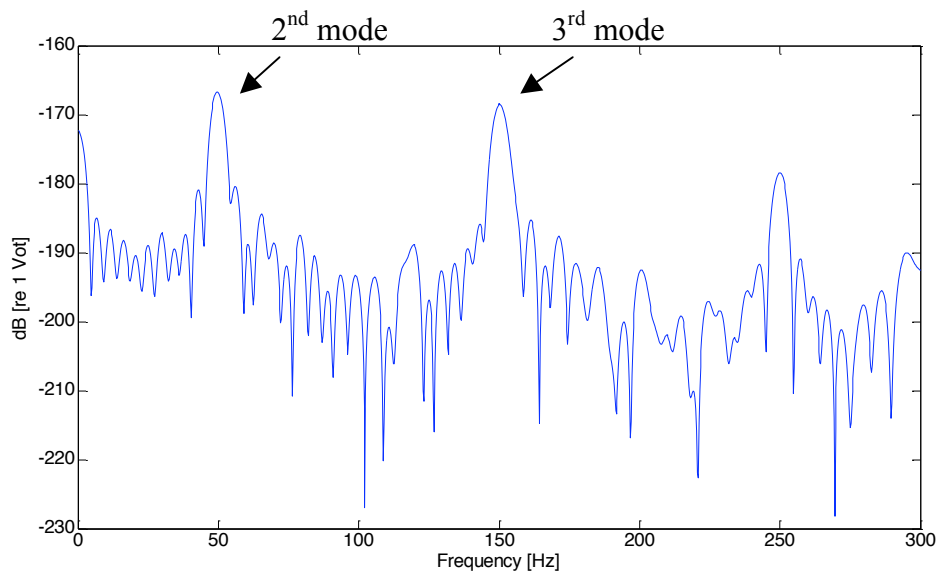


**Figure 4.5 The frequency response of the measurement for modes.**

The basic idea of this method is to find out the first some modes and calculate the Young's modulus by inverting Eq (2.22). Nevertheless, Eq (2.22) have been slightly modified to fit this case. Instead, Eq(4.1) is given the manual and will be used for the calculation of Young's modulus. By using the assumption of last paragraph, the two

modes yield two similar Young's modulus, 7.67 MPa and 8.84 MPa respectively. The average is 8.26 MPa.

However, it is pointed out by Patrik Andersson in the thesis presentation. It seemed more like the amplifier is overdriven, resulting in harmonic distortions at 50, 150, 250 Hz respectively. Plus, it is suggested that one may use the measured impedance at high frequency, as shown in Subsection 4.9, and Eq (3.7) to obtain the bending stiffness  $B$ , then one may have  $E$  if one has  $I$ . But this method will encounter several other problems. First of all, the plate is made of honeycomb, whose unit size and the thickness of every layer is too delicate to be measured, making it difficult to calculate the moment of inertia. One might presume it as an isotropic plate, but the outcome will be slightly erroneous. Secondly, while performing the point impedance measurement, the measurement position is not on the spot of the attached exciter; instead, it is set on the symmetric point on the plate, therefore one cannot use the high frequency simplification (namely Eq (3.2) and Eq (3.3) to calculate the point impedance of the plate. A better solution, suggested by Patrik, is to employ FEM to evaluate the effect of mass loading to the point impedance, although this suggestion is not applied due to the limit of time. Here the author simply again neglect the mass loading at HF to estimate the possible range of Young's modulus. By doing so, it gives the frequency-dependent Young's modulus as shown in Figure 4.6, illustrating that the modulus of elasticity becoming constant at very high frequency, which falls in the range of 6 to 10 MPa. This result is consistent with the result of previous resonant method.

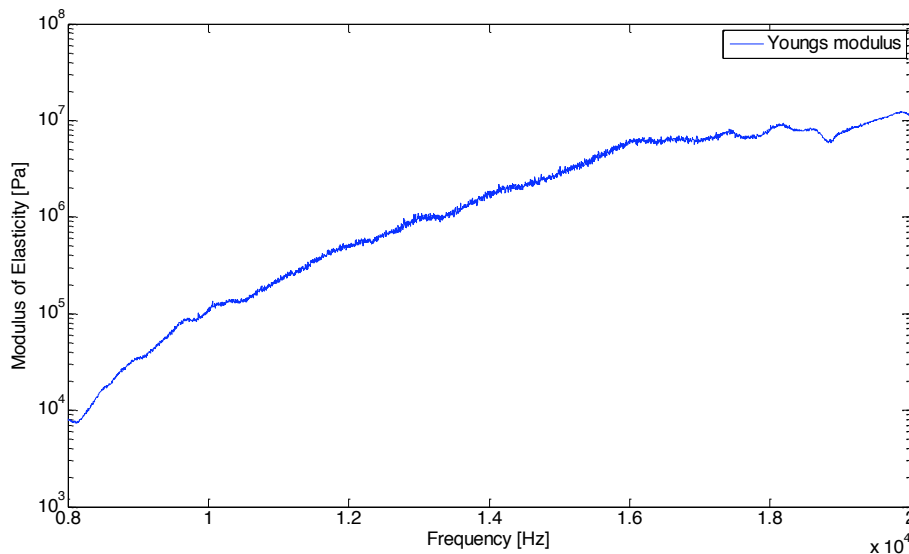


**Figure 4.6 The resultant Young's modulus (modulus of elasticity) by applying Eq (3.7).**

This frequency response can also be used to calculate the loss factor  $Q$ .

$Q$  is defined as:

$$Q = \frac{\Delta f}{f_n} \quad (4.1)$$

where  $f_n$  is the resonant frequency at  $n^{\text{th}}$  mode.

Therefore the resonant frequency  $f_n$  and the effective bandwidth  $\Delta f$  are both needed and they can be found by zoom-in the frequency response, where the effective

bandwidth  $\Delta f$  is defined as the bandwidth in which the magnitude remains less than 3 dB lower than the peak's magnitude.

Figure 4.7 (a) and (b) depicts the zoom-in modes at 50 Hz and 150 Hz respectively.

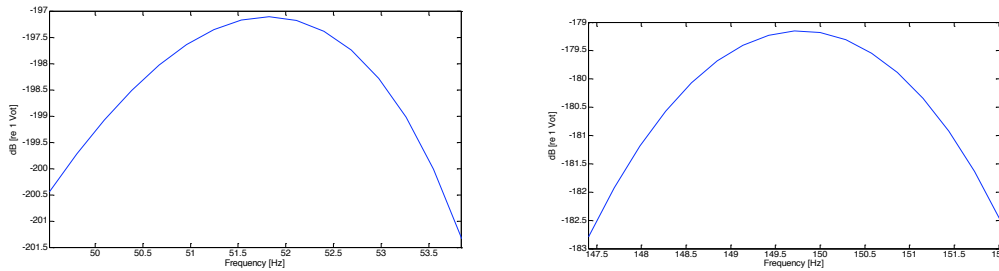


**Figure 4.7 (a) The enlarged 2<sup>nd</sup> mode (b) the enlarged 3<sup>rd</sup> mode**

By using Eq (4.1), the loss factors at these two nature frequencies are obtained, which are 8.33 % at the 2<sup>nd</sup> mode and 3.08 % at the 3<sup>rd</sup> mode.

Additionally, the masses of this test strip and the leftover (plate and exciter) are measured, as well as the dimension; the information of plate and the exciter is therefore acquired. Table 4.1 and Table 4.2 show the measured information and the resultant properties, respectively.

Dimension of the Test Strip	$3.00 \times 13.93 \times 1.2$ [mm <sup>3</sup> ]
Weight of the Test Strip	0.23 [g]
Dimension of the Left Plate	$200 \times 167 \times 1.2$ [mm <sup>3</sup> ]
Weight of the Left Plate (inc. the exciter)	77.3 [g]

**Table 4.1 Measured data of the DML.**

Young's modulus of the plate	8.26 [MPa]
Loss factor of the plate	8.33% at 2 <sup>nd</sup> mode (around 50 Hz) 3.08% at 3 <sup>rd</sup> mode (around 150Hz)
Density of the plate	458.64 [kg/m <sup>3</sup> ]
Mass per unit area	0.5504 [kg/m <sup>2</sup> ]
Weight of the exciter	58.92 [g]

**Table 4.2** Calculated results of the DML's physical properties.

### 4.3 Impulse response and frequency response

The impulse responses of the two loudspeakers are measured by using MLSSA in the anechoic chamber. The upper limit frequency is set to 25 kHz thus it should be accurate for the frequency band under study, i.e. the audible frequency band: 20 Hz – 20 kHz. The distance between the used omni-directional microphone and the loudspeaker is 1 m. Figure 4.8 (a) and (b) show the impulse responses of the objects under study.

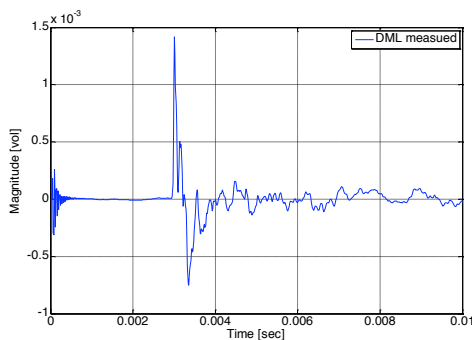


**Figure 4.8 (a)**

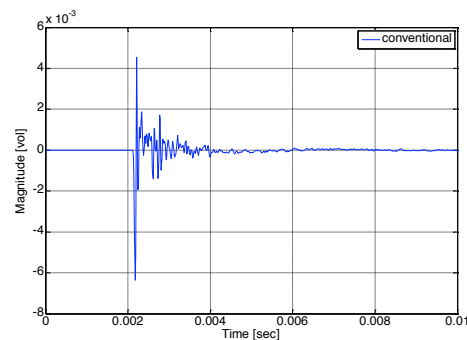


**Figure 4.8(b)**

**Figure 4.8 (a)** The impulse response of DML. **(b)** the conventional loudspeaker in an anechoic chamber.

It is seen in Figure 4.8 (a) that there is an unexpected variation of the magnitude in the 1<sup>st</sup> ms, which appears in almost every impulse response measurement of the DML. It is attributed to the humming of the DML's exciter. Despite the noise, a distinctive difference is noticed between both figures, that the one of electro-dynamic loudspeaker shows a rapid decay, almost dying out just 2 ms after the impulse, while the one of DML displays a long tail, even longer 10 ms after the impulse. This phenomenon can be concluded as the nature behaviour of DMLs. After the impulse, the modes of DMLs still oscillate at their nature frequencies and it takes a while to die out; on the other hand, conventional loudspeakers have less resonances that the

impulse fell faster. Figure 4.9 demonstrates the frequency responses, obtaining from the Fourier Transform of the impulse responses plotted above.

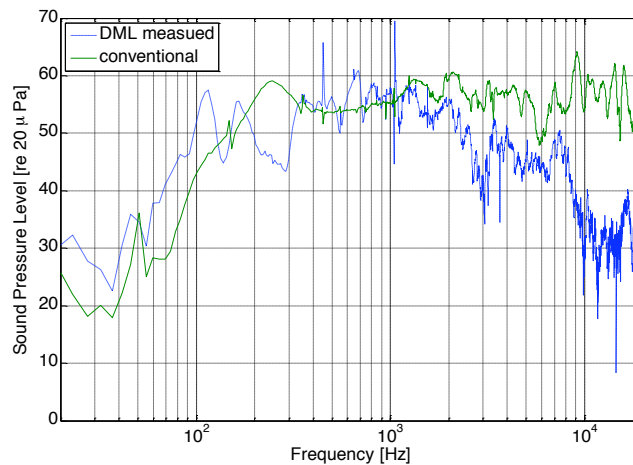


**Figure 4.9** The frequency spectrum of DML and conventional loudspeaker.

It is seen that DML lacks of low frequency while a dramatic drop occurs at 300 Hz and below 300 Hz the SPL is low except two peaks. On the other hand, even though the conventional loudspeaker is in the band of stiffness-control at low frequencies therefore the SPL decreases while the frequency decreases, it still holds relatively higher amplitude than DML until around 120 Hz, which is about the lower frequency limit this size of the multimedia loudspeaker can produce. The lack of low frequency of DML can be attributed to the fact that the modal density is relatively low at low frequencies. As for high frequencies, due to the transformation of bending waves into transverse waves at high frequencies, the SPLs go down gradually. It might be notices there is a rapid descend at 3 kHz, which could be because of the presence of the critical frequency around that frequency.

In contrast to that, the conventional speaker maintains certain magnitude of SPL at high frequencies as high as at middle frequencies, irrespective of the larger variations at high frequencies. For overall behaviours, it is clear that DML shows an obvious modal behaviour that there occur many peaks at corresponding nature frequencies. Since the modes are the responsible for radiating in the design of DML, therefore they are greeted to be seen as many as possible and as evenly distributed as possible, while as for conventional loudspeaker it has been asked as flat as possible.

## 4.4 Directivity

To retrieve directivities, each of both speakers is respectively set on a turn table and a microphone connected to MLSSA system. The microphone pointed to the centre of the speaker under test and the distance between them is set to 1 m. The measurements are done with rotation step of 5 degree. By using the frequency responses, values of certain frequencies of interest could be picked up and the directivities could be obtained. Here, four directivities are presented here, which are 250 Hz, 1 kHz, 4 kHz, and 16 kHz, respectively.

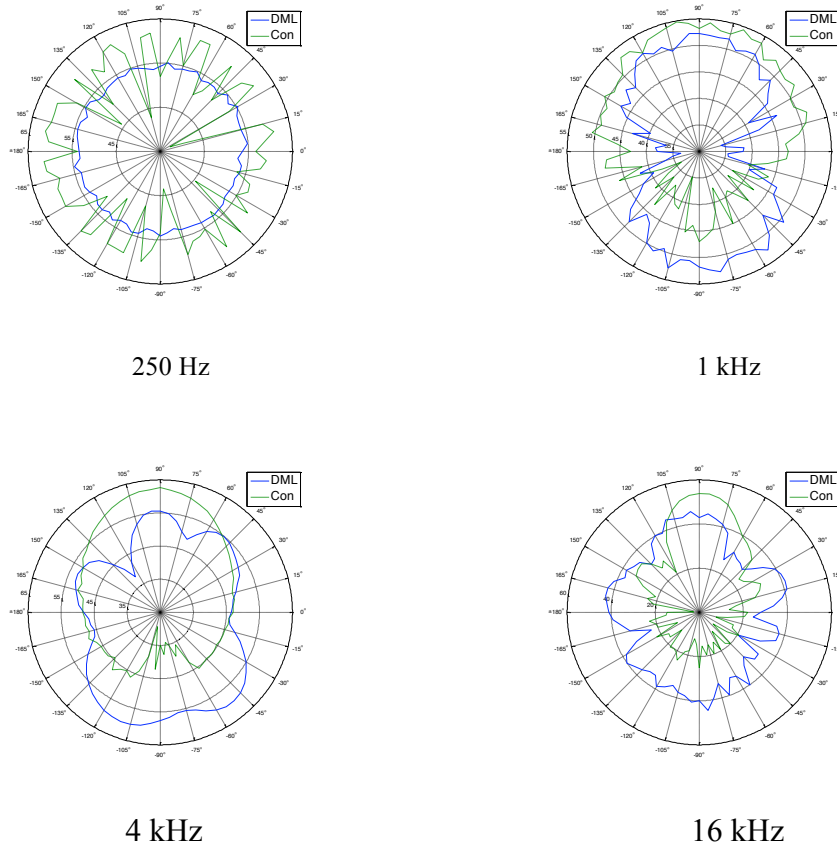


**Figure 4.10 Directional responses of DML and conventional electro-dynamic speaker at respectively 250 Hz, 1 kHz, 4 kHz, and 16 kHz. (In figure, Con stands for conventional speaker)**

As expected, the electro-dynamic type speaker suffers from the beaming problem as the frequency increases. In opposite to that, DML reveals a more omni-directional directivities for all frequencies: it has a nearly perfect circle at 250 Hz and significant dipole behaviour at 1 kHz. However, due to transition from bending waves to transverse waves, it becomes an amoeba-like shape at 4 kHz and maple-leaves like at 16 kHz; however, it basically still remains a round shape. One might also note that at 4 kHz the frontal response (0 to 180 counter-clockwise) is slightly smaller than the rear response, which obviously against the advertisements that the DML’s producer used to say, “DML has a more omni-directional polar response”, at least not the case for middle frequency.

## 4.5 Radiated Sound Power, Efficiency, and Sensitivity

The sound powers are measured by means of diffuse method and the efficiencies are then calculated respectively for the two speakers under test. Another measure indicating how much sound is radiated in terms of sound pressure level, i.e. sensitivity, is also studied in order to give another point of view of sound radiation.

### 4.5.1 Diffuse method for sound power

For the diffuse method, the measurement is carried out in the reverberant room at Applied Acoustics Division in Chalmers University of Technology. A SPL meter of SIP95 is used to measure sound pressure level and the reverberation time. It is done at

6 different positions in order to have a average value. Tab 4.3 demonstrates the averaged reverberation time presented in octave band.

fc (Hz)	63	125	250	500	1000	2000	4000	8000
RT(s)	2.68	1.64	1.62	1.69	1.55	1.35	1.09	0.71

**Tab 4.3 Average reverberation time in octave band. ( $f_c$  stands for centre frequency of the octave band and RT is the reverberation time)**

The sound pressure levels are measured in third octave band and shown in octave band in Figure 4.11.

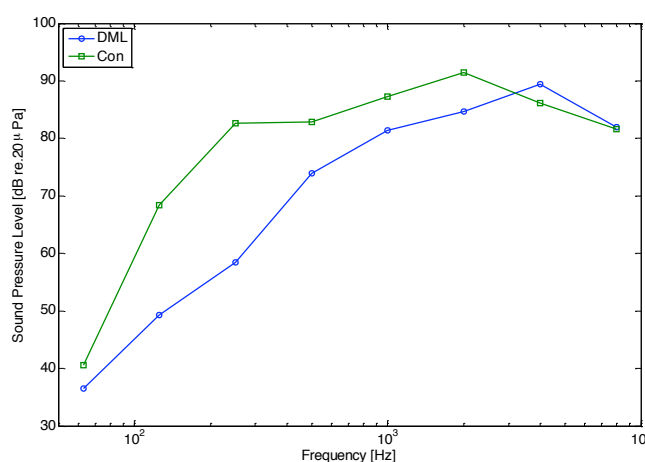


**Figure 4.11 The sound pressure levels of Distributed Mode Loudspeaker and Conventional electro-dynamic loudspeaker.**

The sound power levels are calculated according to the equation below [12]:

$$L_w = \bar{L}_p - 10 \log\left(\frac{T}{T_0}\right) + 10 \log\left(\frac{V}{V_0}\right) - 13 \quad (4.2)$$

Where  $L_w$ : the sound power level;

$\bar{L}_p$ : the mean sound pressure level;

$T$  the mean reverberation time;  $T_0=1$  s;

$V$  the volume of the reverberation chamber;  $V_0=1$  m<sup>3</sup>;

By applying Eq (4.2), the sound power levels are acquired. But since the input electric power can vary for both cases, the effect of input powers should be eliminated by equalizing the sound power to the input powers, which are respectively 0.39 W and 0.28 W for the DML and the conventional speaker. Figure 4.12 exhibits the normalized sound power level, i.e. the sound power levels as the input power is 1 Watt.

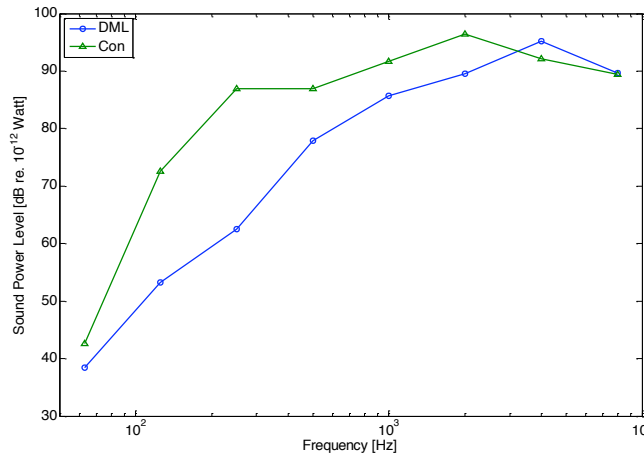


**Figure 4.12** The sound power levels of Distributed Mode Loudspeaker and Conventional electro-dynamic loudspeaker as the input electric power is 1 W, measured by diffuse method.

As illustration in Figure 4.12, the sound power levels of the conventional loudspeaker are much higher than DML's except for the bands above 4 kHz, but it is also observed that DML's sound power levels increase near linearly. That is because for frequencies lower than the DML's critical frequency  $f_c$ , the radiated sound power is independent of frequencies, i.e. constant over frequencies as given by Eq (2.58); while conventional speaker radiates power inverse proportional to frequencies, i.e. descend 6 dB/octave. Please note that Figure 4.12 is presented in octave band, thus the sound power levels of conventional speakers should be constant by theory and the one of DML must be proportional to the centre frequency of each band. This property of sound power distributions will be further demonstrated in later subsection. It might be able to be predicted that DML has the efficiency problem since the sound power level is low in comparison with electro-dynamics'. It is going to be shown later next subsection.

#### 4.5.2 Efficiency

The efficiency is defined as the ratio between the output power and the input power, namely:

$$\eta = \frac{W_{acoustic}}{W_{electrical}} \quad (4.5)$$

The efficiencies are calculated respectively using the sound power obtained by diffuse method and intensity method, as listed in Tab 4.4.

	Efficiency [%]
Distributed Mode Loudspeaker	0.92
Conventional loudspeaker	1.81

**Table 4.4** The efficiency by diffuse method

As displayed in Tab 4.4, it clearly indicates that DML suffers from low efficiency.

### 4.5.3 Sensitivity

The sensitivity of a loudspeaker is usually defined as sound pressure level for a given input of voltage, often 2.83 V r.m.s. The loudspeaker is at on-axis distant as 1 m in the anechoic surroundings [10]. The nominal impedance of 8 ohm is used in MLSSA during the measurement. The sensitivity usually refers to SPL over the audible band, but sometimes also might be specified as the SPL over the octave band centred on 1 kHz. Both results are listed in Table 4.5.

	Distributed Mode Loudspeaker	Electro-dynamic loudspeaker
Overall sensitivity	91.51 dB	98.97 dB
1kHz sensitivity	75.03 dB	78.51 dB

**Tab 4.5 The sensitivities of DML and conventional radiator.**

Unsurprisingly, DML has much lower sensitivity either for overall sensitivity or for 1 kHz sensitivity, which is foreseeable since the efficiency of DML is relatively low.

### 4.6 Distortion

Distortion is the most used measure to describe how well the output can be reproduced with respect to input. Harmonic distortion is the most common way to evaluate amplitude-dependent non-linearity of an audio system. The measurement is done using the setup mentioned in Section 4.4 except the turn table.

The measurement Total Harmonic Distortion, THD, is the ratio of the r.m.s output signal due to distortion, to the total r.m.s value of the output [10]. In this measurement, the input frequency of 1 kHz as the fundamental frequency is employed. The harmonic distortions of both loudspeakers are shown in Figure 4.13 (a) and (b). The amplitude is normalized by dividing the amplitude of fundamental frequency.

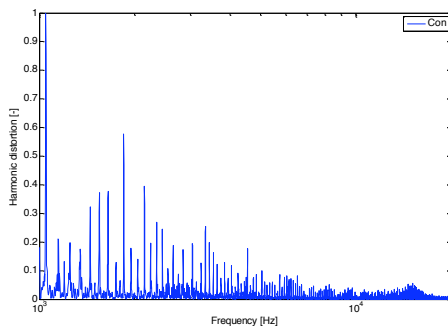


Figure 4.13 (a)

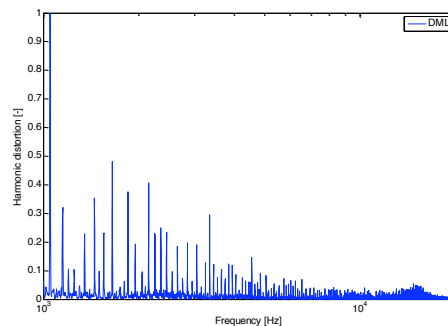


Figure 4.13(b)

**Figure 4.15 The harmonic distortion of (a) conventional radiator (b) DML**

It not easy to judge which one of them has fewer harmonic distortions only by examining the figures. Consequently, the values of THDs are calculated, as tabled in Tab 4.6.

	Electro-dynamic Loudspeaker	Distributed Mode Loudspeaker
THD	13 %	11.07 %
OHD	10.89 %	8.736 %
EHD	7.109 %	6.8 %

**Tab 4.6 The total harmonic distortion (THD), the odd harmonic distortion (OHD), and the even harmonic distortion (EHD) of electrodynamic speaker and DML.**

Note that these measurements in fact also include the system noise, therefore often denoted as “THD + N”, N for noise.

One can notice that DML is lower no matter in THD, OHD, or EHD. Lesser the harmonic distortion, more accurate the sound the speaker can produce. An interesting thing of EHD is that it sometimes facilitates the listening experience. The most famous example is vacuum tube amplifiers.

Another unusually phenomena needs to be pay some attentions here is that there are sub-harmonic occurred in the measurement, which usually happens as the non-linearity of the system is asymmetric. The sub-harmonic of DML is presented in the following Figure 4.14.

Note that some sub-harmonics such as the one at 450 Hz even is with the magnitude twice as the magnitude of the fundamental frequency.

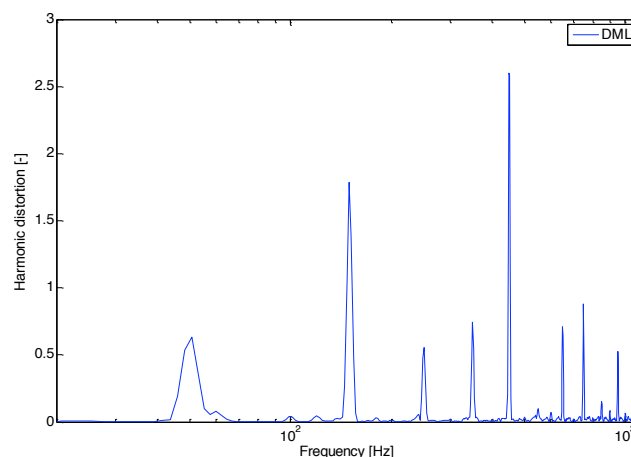


**Figure 4.14 Sub-harmonics of DML as the fundamental frequency is 1 kHz.**

## 4.7 Test on the Diffuse Sound of DML

In this subsection, a simply test is accomplished to investigate the how diffuse the sound that DML produces. It is known that DML can be thought of the combination of infinite modes which radiate independently in time and space. Thus if the DML is divided by several parts, these sub-DMLs should be independent to each other. In this test, it is divided by two parts, the lower part and upper part by masking the other half by a big baffle with absorbers. Afterward, the sound pressures of these two parts are reunited respectively by the assumptions of that they are absolutely incoherent or they are totally coherent. By comparing these two results with the measurement of on-axis free field sound pressure, one will see if the sounds of DML are more like fully incoherent or coherent. Figure 4.15 reveals the results, which is not easy to be observed. Thus it is presented in one-third octave band, as Figure 4.16.

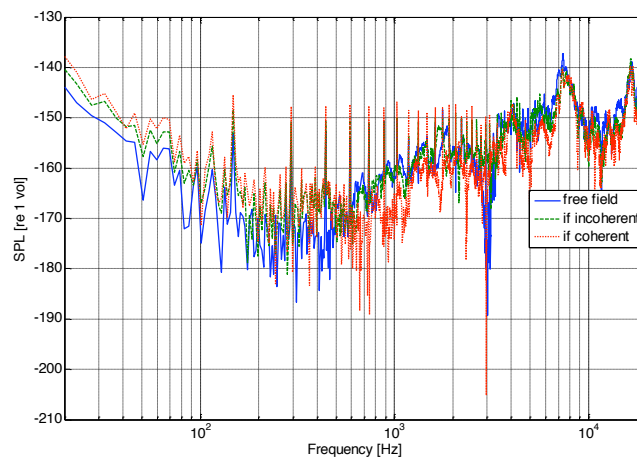


**Figure 4.15** Sound pressure levels comparison between the SPL under the assumption of incoherent, the SPL under the assumption of coherent, and the free-field.

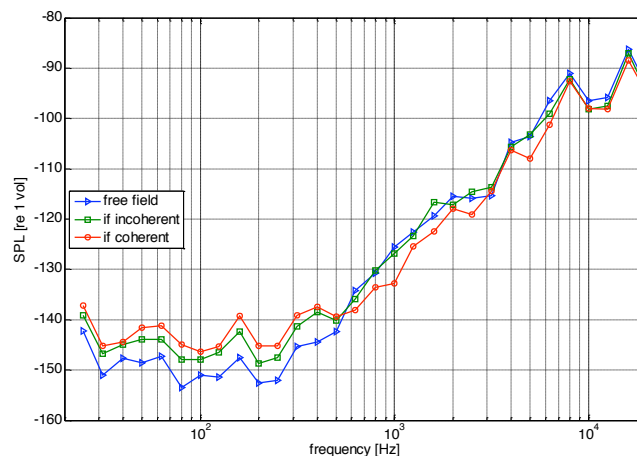


**Figure 4.16** Sound pressure levels comparison in 1/3 octave band between the SPL under the assumption of incoherent, the SPL under the assumption of coherent, and the free-field.

It is noticed that at the centre frequencies above 630 Hz, the curve of free field and the one of the incoherent assumption matches very well, while the difference between free-field and the coherent assumption becomes distinctive at the same frequency band. However, at low frequencies, even the SPLs of incoherent surmise is still closer

to the fee-filed's than the values of coherent presumption, but the variation is remarkable. This can be explained that the absorber of the baffle has less effect for low frequencies, causing low frequency leakage by transmitting through the baffle while the measurement of half baffled DML is performing, which implies that the measured low frequencies would have higher amplitude than expected.

## 4.8 Sound Pressure Level Distribution

So far, all the tests are performed in the anechoic chamber to avoid the effect of reverberation. Nevertheless, speakers are barely used in anechoic environment, instead, usually used in the place with reverberations. Therefore, the study of the performance of these two speakers in an ordinary listening environment is essential. Consequently, the lecture room of Applied Acoustic Division in Chalmers University of Technology is chosen to carry out a series of measurements. The lecture room has the length of 7.8 m, width of 5.08 m and height of 3.62 m. The reverberation of the lecture room is shown in Tab 4.7 (average of 5 different RT measurements).

	125 Hz	250 Hz	500 Hz	1 kHz	2 kHz	4 kHz	8 kHz	Overall
RT	0.8136	0.5794	0.4824	0.5652	0.6514	0.6422	0.5472	0.5248

**Tab 4.7 The reverberation time of each octave band, up to the band centred at 8 kHz**

Two different measurements are performed. In the first measurement, a dummy is used and two microphones are inserted into the ear holes of the dummy in order to perceive the binaural impulse responses. The use of head and torso is to take the effect of human body presented in sound field into account. The dummy is placed on the chair and the height is adjusted to a standard height of a human being. The measurements are executed at 15 different positions. See Figure 4.17 for details.

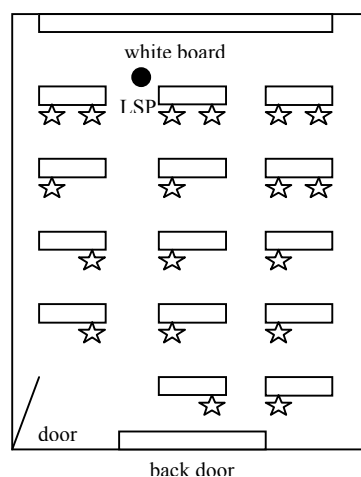


**Figure 4.17 The measurement positions (mark by stars) of binaural impulse response and the black dot stands for the position of loudspeaker.**

The 15 pairs of impulse response are used to calculate room acoustic matrices which describe the acoustic properties of a room. Tab 4.6 shows the matrices for the two speakers under test.

	IACC	D50
Electrodynamic	0.4308	88.91
DML	0.2002	86.56

**Tab 4.6 The acoustic metrics using respectively the electrodynamic speaker and the DML (average of the 15 measurements).**

Of course these matrices are also influenced by the radiation properties of speakers. The outcome of the average IACC obeys the expectation that the IACC obtained by DML would be lower than the one obtained by electro-dynamic speaker due to DML's nature of diffuse field. The frequency responses shown in Section 4.2 imply that DML lacks of low frequencies and high frequencies, thus the fact that other matrices of DML listed in Tab 4.6 are also lower than conventional speaker is predictable.

The second measurement is mainly aimed to investigate the sound pressure distribution in the classroom. Instead of binaural microphones, only one microphone is used for measurement. The height of the microphone is 1.3 m from the ground. The lecture room is divided into 6 X 9 blocks by the step of 1 m. To avoid strong reflection, the positions near the wall are not measured, leaving 4 X 7, 28 measurement positions, as plotted in Figure 4.18.

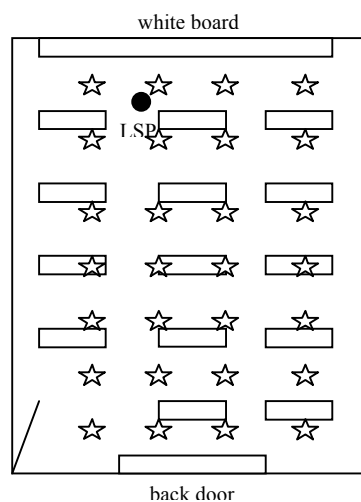


**Figure 4.18 The measurement positions (marked by stars) for obtaining the sound pressure distribution.**

Figure 4.19 (a) and (b) show the contours of the sound pressure level distributions of electrodynamic speaker and DML in the octave band centred at 250 Hz. In Figure 4.20 (a) and (b), the centre frequency is 1 kHz and it is 4 kHz in Figure 21 (a) and (b).

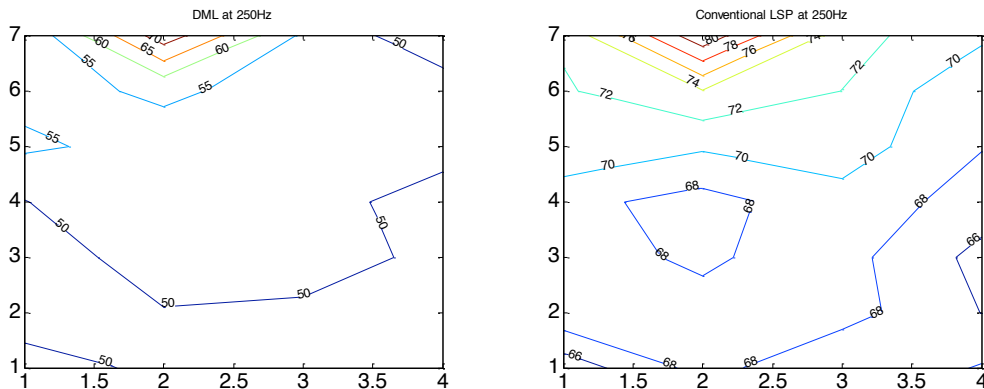


**Figure 4.19** The SPL distributions of (a) DML (b) electrodynamic speaker at 250 Hz

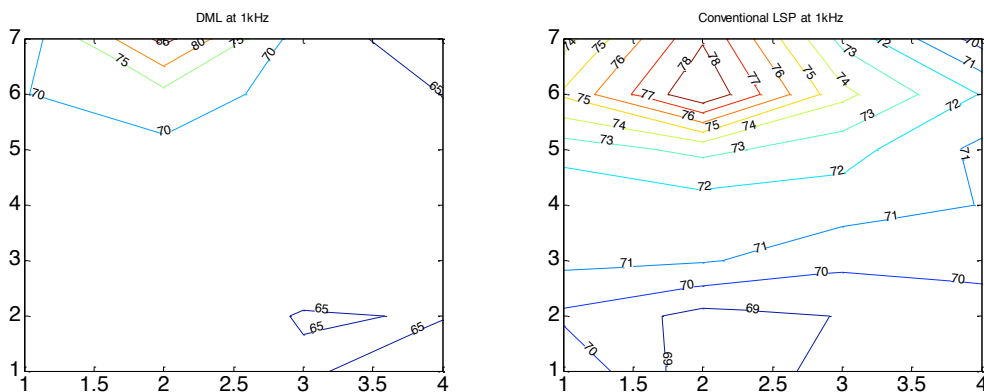


**Figure 4.20** The SPL distributions of (a) DML (b) electrodynamic speaker at 1 kHz

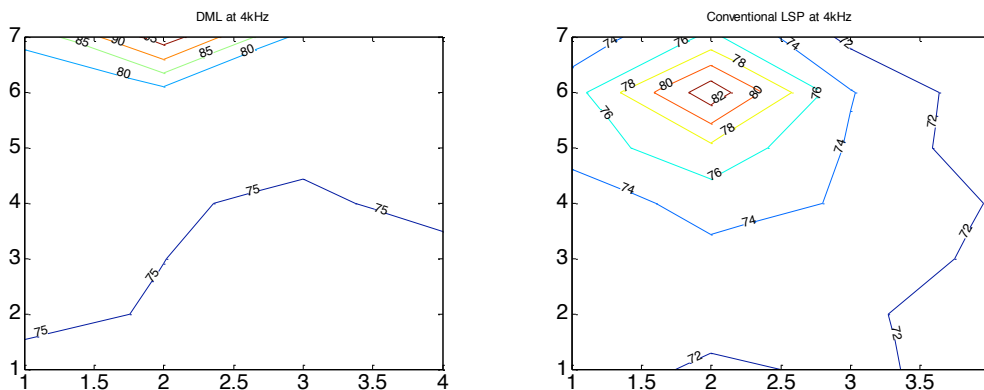


**Figure 4.21** The SPL distributions of (a) DML (b) electrodynamic speaker at 4 kHz

It is noted that no matter for which frequency, DML produced a much more even distributed sound field. It can be attributed to its nature of producing diffuse sound. This implies that the listening positions nearly not affect the perception of sound, meaning audiences can sit almost every spots without feeling much difference; on the other hand, there is always a so-called “sweet spot” while using the conventional loudspeaker and the listening environment usually needs to be treated carefully to achieve the best performance on sweet spot, which is unnecessary for DML.

## 4.9 Mechanical impedance

The mechanical impedance is often of interest because it reveals the physical properties of the device under test. For DML, it employs the panel for reproducing sound, thus the response, usually the velocity, of the plate for a given force becomes significant. Impedances are generally classified by two groups: driving point impedance and transmitted impedance. Driving point impedance, or point impedance, is especially of interest.

The best position to measure the point impedance would be the position of the exciter because one can reason out the velocity while excited by the exciter if one knows the point impedance of exciter's position; however, the exciter is firmly attached to the panel that removing the exciter might cause the damage to the panel as well. Thus another position symmetric to the exciter is measured instead. If the panel is ideally uniform and the effect due to the presence of the exciter can be neglected, then the point impedance of measured position should be identical to the point impedance of the exciter's location, refer to Figure 4.22.

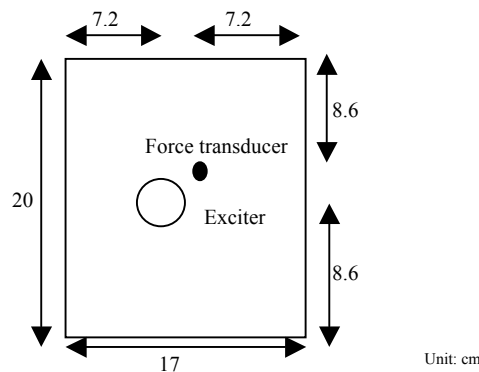


**Figure 4.22** The locations of measurement position and the exciter of the panel. The black dot is the position of the force transducer and the circle is the exciter.

A force transducer is utilized to excite the plate and measure the input force. The force transducer is well attached to the panel by using X60 glue, therefore the measurement would be accurate up till several kHz while the upper limit frequency is only few hundred Hz using wax. A Laser Doppler Vibrometer and an accelerometer are used to measure the velocity. The force transducer and the accelerometer are both connected to a charge amplifier which transforms the signal measured into the voltage the acquisition station can read. Then the impedance  $Z$  could be obtained by applying following definition:

$$Z = \frac{F}{V} \quad (4.6)$$

where  $F$  the force,  $V$  the velocity.

But prior to seeing the impedance, one needs to take a look on the coherence between the force and the input signal, as displayed in Figure 4.23, to understand the quality of the measurement and the upper frequency limit of available data. As one can see, the coherence started falling since 6 kHz and become less than 0.9 around 8

kHz, suggesting that the data after 8 kHz is not in good quality and one should not show the data above the rim.

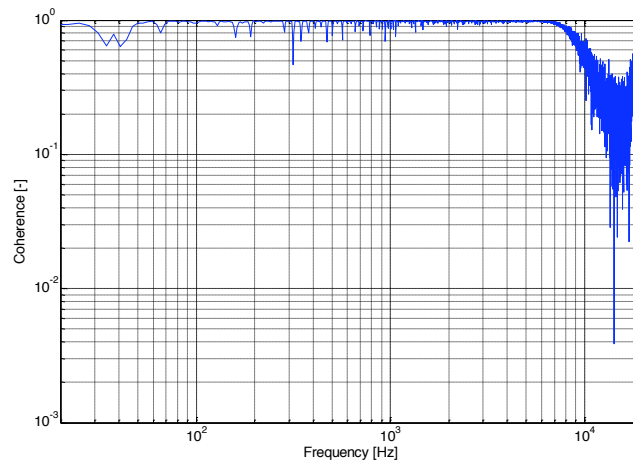


Figure 4.23 The coherence between the force and the input signal.

The measurements are performed twice; in the first time only LDV is used while in the last time LDV and accelerometer are both employed. Figure 4.24 illustrates the point impedance measured only with LDV.

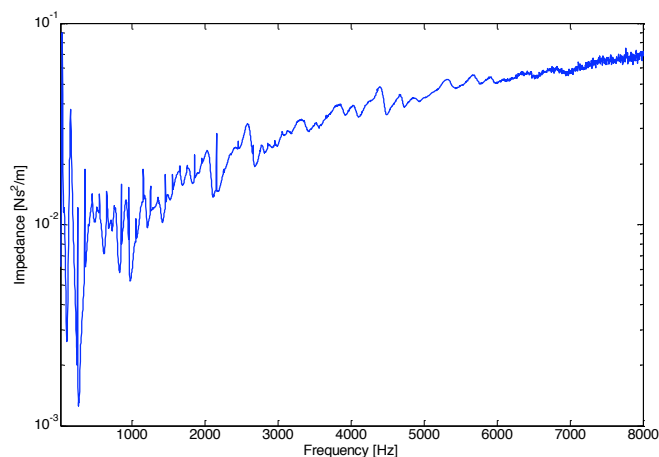


Figure 4.24 The point impedance measured by LDV.

It is seen that the point impedance is not a constant as the theory suggests. The measured driving point impedance increases gradually with frequency. This is due to the mass loading from the attached exciter. The exciter resulted in a discontinuity, causing reflections and perhaps new modes between the force transducer and the exciter. On the other hand, the theory says that the point impedance is proportional to the square root of the area density of the panel but due to the presence of the exciter, the mass is not evenly distributed over the surface thus the theory does not apply for this case.

In the second driving point impedance measurement, the accelerometer is also used on the other side of the panel and the laser beam of LDV is focused on it. The result

measured by accelerometer and LDV are plotted in Figure 4.27, as well as the result measured only with LDV for comparison.

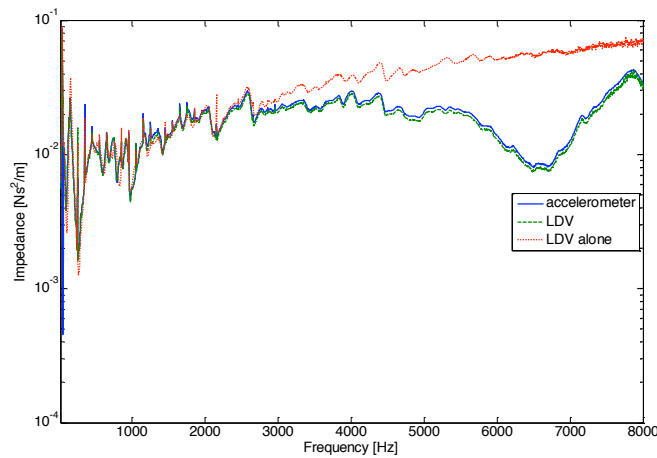


Figure 4.25 The point impedance measured by accelerometer and LDV. LDV alone stands for the result measured only with LDV.

Clearly one can observe that the accelerometer and the LDV almost got the identical results. The difference between these two is minor. It is also noticed that the point impedance measured with the presence of the accelerometer, no matter the one by LDV or accelerometer, is more like constant as the theory predicts, irrespective of the variation after 5 kHz. The only difference of the curve of “LDV alone” and “LDV” is that while performing the measurement of “LDV”, it is equipped with the accelerometer and not the case in “LDV”. Clearly, the drop at 5 kHz is due to the presence of accelerometer.

In addition, it might be interesting to see the transfer function of the exciter. Thus the velocities while using the exciter are measured in two different ways. The first method is to assume the middle point of the exciter can represent the exciter; therefore the measurement is performed on the middle point of the exciter. The second method is simply to scan the surface the exciter, 180 points, and take the spatial average.

The transfer function is calculated by the assumption that the driving point impedance on the exciter is same as the one on the symmetric point, as Figure 4.24 and Figure 4.25. The outcome is drawn in Figure 4.26.

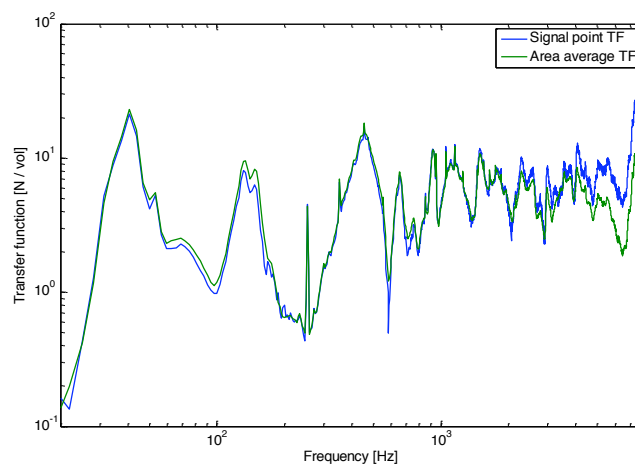


Figure 4.26 The transfer function of the exciter.

It is observed that the measurement of signal point on the middle of the exciter can represent the average measurements of the exciter very well up to around 5 kHz.

## 4.10 An example of a commercial DML exciter

Another commercial product of Distributed Mode Loudspeaker is studied here, or more precisely, a portable exciter of Distributed Mode Loudspeaker. The exciter is round with the diameter of 2 cm, which is powered by a battery package - 2 AAA batteries are needed- and amplifier complex. The photos are shown in Appendix D1.

It is attached to respectively a paper foam plate with the radius of 10.5 cm and the SPL is measured, as shown in Figure 4.27.

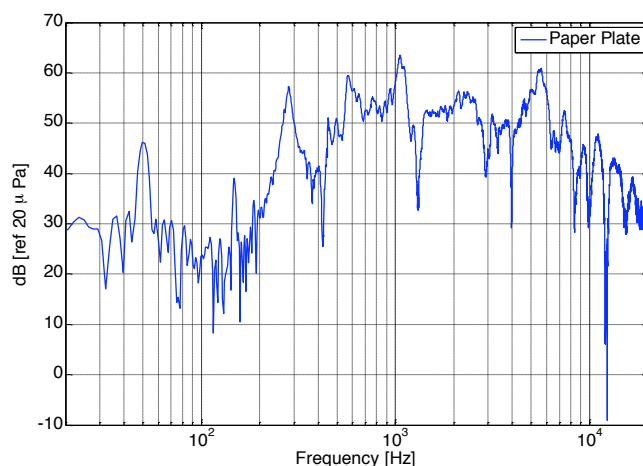


**Figure 4.27** The sound pressure level of the paper plate excited by the portable exciter.

As one can foresee, the SPL at low frequency is low due to the limit of the size. As for higher frequency, there are some severe instant drops and remarkable resonant peaks which suggest that it will not sound very well. The subjective listening test of the author gives an affirmative result, but somehow acceptable if one does not expect too much.

## 4.11 Listening test

A listening test is performed to study the subjects' response to DML and conventional speaker. The test sounds are produced by using binaural impulse responses, as done in Section 4.8, to perform the convolutions with five different types of music. The binaural impulse response recorded in the lecture room contains the sound field properties; on the other hand, these clips of music are recorded in an anechoic circumstance therefore they contain nearly no environment effect. Consequently the convolved clips of music can be regarded as recorded in the lecture room. The music clips include clips of piano, drums, speech, cello, and symphony. The convolution process is as illustrated in Figure 4.28.

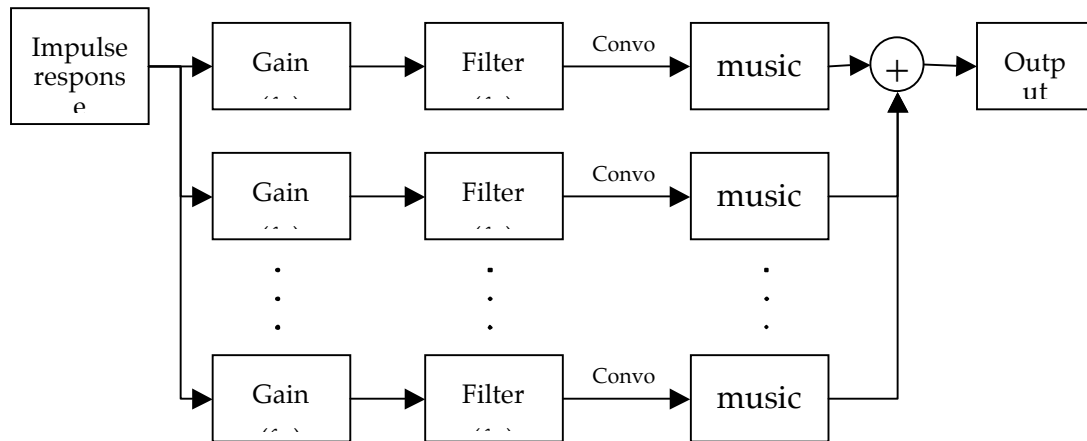


**Figure 4.28** The structure of convolution process, where  $f_{cn}$  denotes the centre frequency for the  $n$ th 1/3 octave band.

The gains **Gain** ( $f_{cn}$ ) are set respectively in accordance with the r.m.s value of each band. As matter as fact, they are the reciprocal of the r.m.s value therefore after the convolutions each band will contain the same r.m.s value. The band-pass filters are employed to filter out the unwanted information, i.e. the data outside that 1/3 octave band.

One may think that to adjust the amplitude of every band directly is easier than using the complicated process of Figure 4.26. However, while the author tried to do so, it turned out with annoying noise, which could be because of the discontinuities at the boundary for the two adjacent bands. Nevertheless, by applying the structural processes of Figure 4.31, the discontinuities are properly smoothed therefore one will hear no notable noise or humming.

Twenty subjects had attended this test. The used questionnaire is partially shown in Appendix A.1 (the repeated parts are neglected) and the information of the subjects are drawn Appendix A.2

This listening test had been divided by two parts. In the first section, the audiences will hear 50 individual clips of music, comprised by 25 pairs of sound but will not appear in pairs; instead, they will show up randomly distributed in these 50 clips. Each pair consist one sound made by convolving the impulse response using DML and a certain music clip and the other sound using conventional electro-magnetic speaker. These two couple impulse response are randomly picked up from the measurements at the same spot in Subection 4.8. The subjects needed to answer a series of questions as shown in Appendix A.1. Part I after listening to each clip of music. The scores of preference in the last question for both types of loudspeakers are accumulated respectively for each subject to find out the preference. The consequence is shown in Table 4.7. The total number of people is only 16, one may notice. This is due to an accident that the playlist used for these four subjects is missing, making the result of these 4 persons inapplicable.

Types of loudspeaker	DML	Electrodynamic	The same
Preference votes (people)	7	7	2

**Table 4.7 The preference for DML and electrodynamic loudspeaker in Part I of the listening test**

In Part II, it is basically as in Part I, 25 pairs of music are employed; nevertheless, the paired clips are played in pair in this section. The subjects are supposed to choose the one they prefer and give the difference of preference. As done previously, the scores are summed up to see the subjects' fancy to these two loudspeakers, as shown in Table 4.8.

Types of loudspeaker	DML	Electrodynamic
Preference votes (people)	12	8

**Table 4.8 The preference for DML and electrodynamic loudspeaker in Part I of the listening test**

Table 4.7 and Table 4.8 reveal that after equalization DML's performance is slightly better than electrodynamic speaker, at least subjectively. Since this process of equalization basically solves the problems of lack of certain frequency band; therefore it is ruled out from the factors affecting the performance. The possible reason letting DML sound better is the impulse response has a long tail, leading a more diffused sound field and probably leading to a better vividness. This result also hints that the performance of the DML could be improved by the use of a DSP.

## 4.12 Diaphragm Scan

Besides, a full scan using LDV is performed on the DML by using the same setup as used for mechanical impedance measurement. 291 positions are measured to represent the diaphragm of DML and it is done 5 times at each position then took the average. The function of making animation of PSV software helps to pick up certain frequency band, calculate the peak in this band, and animate the displacement of the plate. This is particularly helpful for modal analysis. Figure 4.29 exhibit several frames of the animation while the frequency is at 47 Hz. It should be the second mode, which accords with the result in the Young's modulus measurement, ref. Section 4.2.

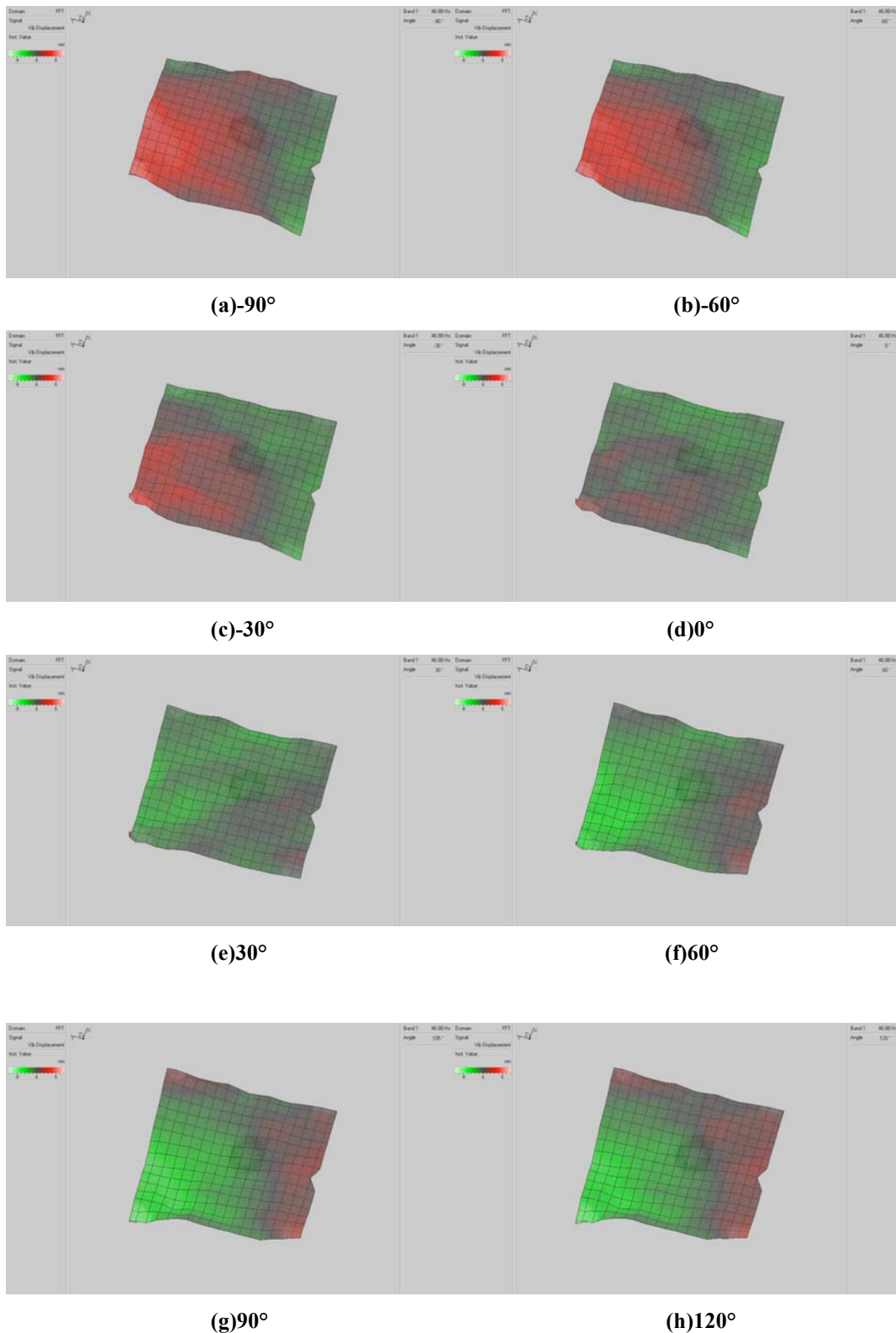


**Figure 4.29 (a)~(h)** The frames of the animation at 47 Hz, where the degrees represent the phase of time.

To avoid being cumbersome, the rest is not shown here. One clearly can see the modal behaviour here: the resonant peak has appeared in the left down corner in and gradually disappeared with time. Many other animations had been made at different frequency range or by using different sound source; however, due to the limit of

printed report, they are not be able to be fully exhibited here. One interested to see these result may contact the author.

## 5 Simulation and Optimization

As per the previous chapters, DML produces sounds by exciting the modes of the attached plate; therefore the performance of DML can be optimized by optimizing the modes. One often wants a plate with evenly distributed modes to cover all the frequencies of interests. Recall Eq (2.21). It is obvious that the mode frequencies are influenced only by the ratio of the bending stiffness to the mass per area and the size of the panel. But one should not forget that the position of the exciter is also essential since it decides which modes will be excited.

### 5.1 Optimization of length / width ratio

For a given plate with fixed surface area, the ratio of the length to the width of the plate will be the key factor to affect the modes and their performance. The goal of optimization here is set to have the most evenly distribution of the modes, consequently the ratio of the length to the width is varied from 0.01 to 1 by the step of 0.01 and the modes are calculated for each cases. The definition of “the most evenly distribution of modes” is to minimize the variance of the nature frequencies for the first some modes, 2500 here.

The ratio with the most evenly distribution of modes is found and the nature frequencies of this specific ratio versus the numbers of the modes are plotted in Figure 5.1 along with the other ratios’. Note that there is so-called “golden ratio”, about 0.9482, suggested by NXT is also presented in Figure 5.1.

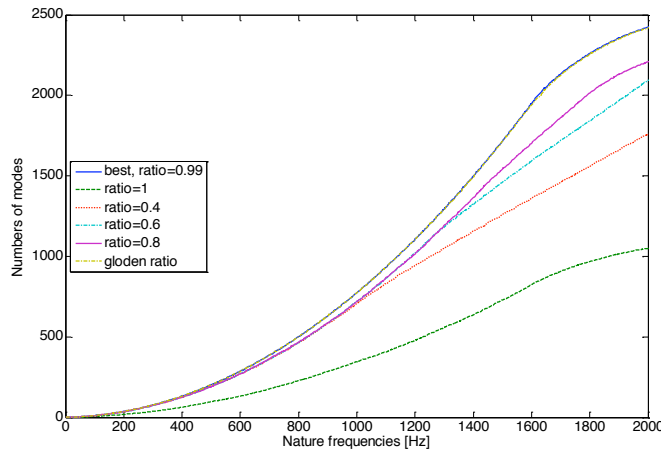


**Figure 5.1** The nature frequencies versus number of modes of different ratios of length to width.

As one can observe, the numbers of modes basically increase as the ratio increases in the fixed frequency band and it reaches its maximum values as the ratio is 0.99, the optimized ratio one might obtains. The advised golden ratio reveals almost identical curve to the optimized one. The main difference of golden ratio and the optimized one is mainly in the concerns of optimization; only length/ width ratio is varied here as the golden ratio is obtained by trading the length / width ratio and the excitation position. Regardless the factors of consideration, the golden ratio seem like a safer choice. The reason is that 0.99 is quite close to 1. If one looks at the curve of ratio =1, one will realize how dramatically drop it is just from 0.99 to 1, and this is very possible to

happen due to the inaccuracy of cutting. To avoid this problem, one should choose a ratio which is not close to 1 but still has an even modes distribution, e.g. 0.95, namely the golden ratio.

## 5.2 The dimension's effect to DML at low frequency

It is shown in Subsection 4.3 that at low frequency, especially below 300 Hz, the sound pressure level is relatively low. That is because of fewer modes are of presence in low frequency range. Therefore, it is institutively to increase the modes at low frequency, or put in another way, lower the nature frequency of the first mode. Eq (2.21) gives hints how to do so. Of course, one can select a heavier material, or make the plate thicker; however, either way will cost of radiated power and efficiency as mentioned previously, refer to 2.4.3, and that is one does not want to see. A better way is magnify the plate of DML. By this way, one will not need to pay for the reduction of radiation, but still make the low frequency response improved.

Due to the inconvenience of varying the size of the plate physically, Comsol Mutiphysics is utilized to investigate the effect of the length and width to the low frequency response. The used material information is shown as Table 5.1

Young's modulus [Pa]	$2 \times 10^{11}$
Density [ $\text{kg/m}^3$ ]	7850
Poisson's ratio	0.33

**Table 5.1 The material properties of the material used in Comsol's model**

The model employed sound-structure interaction mode and the size of the plate in the model is identical with the size of the DML's panel. The plate is surrounded with air of 1 m radius, as Figure 5.2.



**Figure 5.2 The sketch of Comsol's model, where the rectangular plate is the DML and the three circles represent the air sphere**

The size of mesh needs to be carefully defined to fit the criterion that there must be at least 6 meshes per wavelength. This requirement has limited the applicable frequency range since higher the frequencies, more meshes are needed and longer calculation time it will consume. That is why in these simulations of 5.2, 5.3 and 5.4, the upper frequency limit are often quite low, mainly in the low frequency range.

In this case, the upper limit of frequency is set as 300 Hz. After a long computation, this model will give the sound pressure level for every slice, which can be used for directivity analysis, as Figure 5.3.

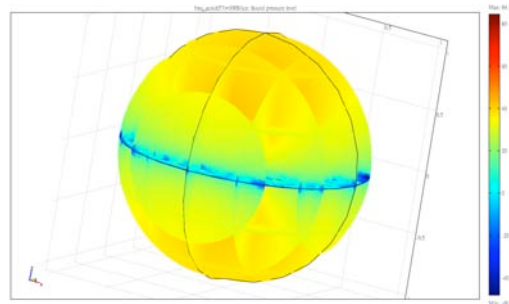


**Figure 5.3 Result of Comsol's model.**

However, in this simulation, the polar responses are not concerned; the more important thing is the on-axis frequency response in the anechoic surrounding. Therefore, the SPL at the position 1 m away from the middle point of the plate is drawn as the area size of the plate have increased integral times bigger. Figure 5.4 illustrates the result; it is clear that as the panel's area increase, there will be more modes at low frequency, resulting flatter frequency response.

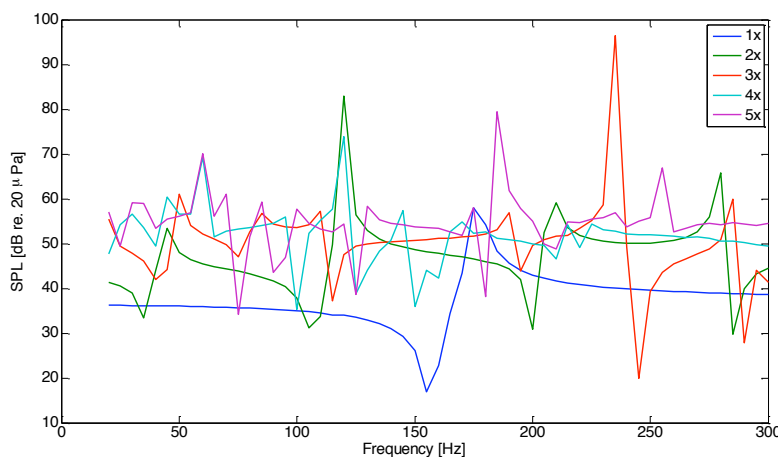


**Figure 5.4 The low frequency response for the plate with different surface area. The integral denotes the how many times bigger the plate relative to the original one is.**

### 5.3 The boundaries effect to DML

Beside the simulation in 5.2, this FEM model is also used for clamp analysis. It is very easily to reason out theoretically that the types of boundary facilitating rotation will be better choices, such as roller or simple supporting. Figure 5.5 reveals the simulated result at LF. In the simulations, the clamps available in Comsol Mutiphysics including roller, free, and fixed are used to vary the boundaries. One can see the result agree with the expectation: the case with fully free boundary shows the most obvious resonance while the one with fully fixed edge behave oppositely. The partly roller one has no anti-resonance, which can be seen as mediocre but most practical. It is also noted that fully roller one gives a very flat frequency response, suggesting that one may try to use this way of clamping if one want an even spectrum. Another phenomena one need to notice is the SPL is relatively low with respect to the

cases with resonances and the spectrum slowly descends in Figure 5.5. Therefore, this hypothesis needs to be confirmed by practical experiment or the simulation up to higher frequencies, and it is not a DML anymore if it is the case.

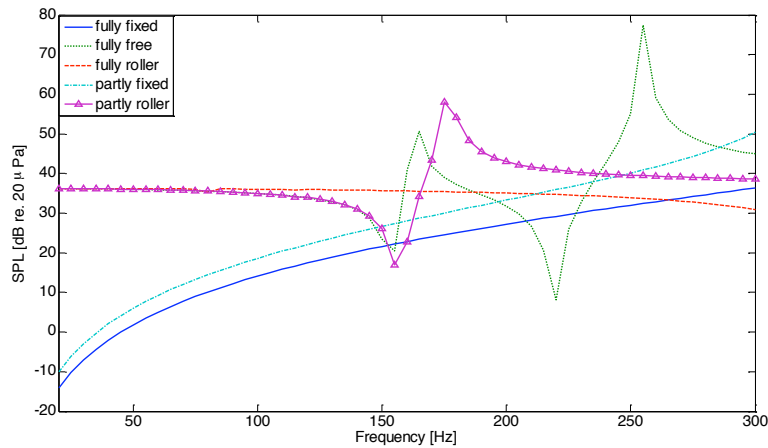


**Figure 5.5** The clamps' effect to a DML at LF, where “fully fixed” denotes the four edges are fully fixed and “partly fixed” means the longer side of the DML is fixed. The same idea applies to the rest conditions.

## 5.4 DML model using measured material properties

The material properties in the model, as Table 5.1, are replaced by the measured mechanical characteristic listed in Table 4.2. However, the Poisson's ratio is not measured therefore it remains default value, that is 0.33. The simulated result is shown in Figure 5.6 along with the measurement. Despite the level difference, the behaviour of both curve are quite similar: the resonant peak and drop have appeared roughly at the same frequencies and the trends are also alike. It is believed that the spectrum will fit the measurement if the Poisson's ratio is given.

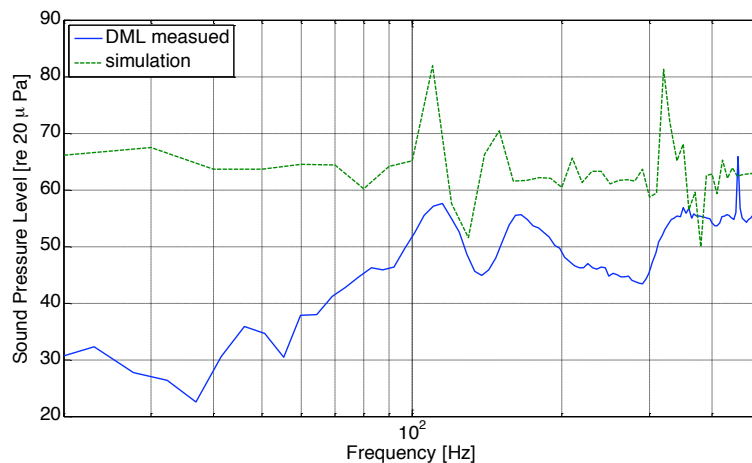


**Figure 5.6** The frequency response of the simulation of DML using measured physic properties, along with the measured SPL.

## 6 Conclusion

In this thesis report, Bending Wave Loudspeaker and Distributed Mode Loudspeaker, the two common types of loudspeakers employing bending waves are introduced and reviewed, especially for DML. By examining the result of IACC and the SPL distribution in a well-damped surrounding, the property that DML is with diffuse sound field is confirmed. It is also seen that DML does have a less directional response in most of the frequency bands; however, it may not be true in middle frequency, as shown earlier. The spectrum also expose that DML has problem at low and high frequencies. The outcome of sensitivities and efficiencies unearh that DMLs have suffered from low sensitivities and efficiencies.

In addition, the listening test unveils that after equalization the audiences may prefer DML to electro-dynamic loudspeaker, since the problem of lacking low and high frequencies has been fixed by equalization, which also give a possibility that one may improve the frequency response by the use of an equalizer.

The simulations also pointed out the effect of the ratio of length/width to the modal density, saying that the length and width should never be the same for the sake of modal optimization and one may have the best ratio by simulation. Plus, the modelling using Comsol Mutiphysics also demonstrates how the SPLs at LF are ascended by prolonging the length and width of the panel and how the clamps influence DML's performance.

In short, DML still has a long way to go to be as satisfiable as the conventional electro-magnetic loudspeaker in practice.



## 7 Suggestion for future work

The result of listening test suggests that the sound quality of DML may be improved by using an equalizer. Therefore, one may use a real time equalizer while measuring the frequency response, in order to examine if this way of improving does work. It is also suggested by Prof. Mendel Kleiner that the lack of low frequency of DML can be compensated by mounting the radiator into a box.

One might doubt the sample cannot represent all DMLs' performance, not to mention this sample is the one while DML is introduced at the first time. Therefore one is encouraged to collect more numbers of DML and had better collect the latest ones. It is also questioned that DML may have worse response in a more reverberant surrounding. Thus one can perform some measurements in such circumstances to clear this question up.



# Bibliographic

- [1] Dicks Dipole Drive, German Physiks, <http://www.german-physiks.com/technology/the-ddd-driver.html>
- [2] 80Hz - 35kHz, Manger speakers, <http://www.manger-audio.co.uk>
- [3] Rodrigo Martinez Redondo, *Optimization of Bending Wave Loudspeaker*, Chalmers University of Technology, Department of Applied Acoustics, Master Thesis 2007:38, Gothenburg, Sweden.
- [4] L Cremer, M Heckl & EE Ungar. *Structure-borne sound*, Springer Verlag, Berlin, 1988
- [5] Göbel High End, <http://www.goebel-audio.de/en/company/techno2.html>
- [6] Cai Brockmann, *Göbel Audio Detaille S and Detaille Sub*, [www.goebel-audio.de/en/support/goebel\\_image\\_hifi.pdf](http://www.goebel-audio.de/en/support/goebel_image_hifi.pdf)
- [7] Panzer and Harris, N, *Distributed-mode loudspeaker radiation simulation*, 105<sup>th</sup> AES Convention, San Francisco, September 1998, preprint 4783.
- [8] Mingsing R. Bai and Talung Huang, *Development of panel loudspeaker system: Design, evaluation, and enhancement*, Acoustic Society of America.
- [9] John Borwick, *Loudspeaker and Headphone Handbook*, Focal Press, 2001.
- [10] Bank G, *The intrinsic scalability of the distributed mode loudspeaker*, 104th AES Convention, May 1998, preprint 4742.
- [11] Panzer, J and Harris, N, *Distributed-mode loudspeaker simulation*, 105<sup>th</sup> AES Convention, San Francisco, Sep 1998, preprint 4783.
- [12] *ISO 3743*, Chapter 8-2.
- [13] MLSSA reference manual, version 10WI, Rev 8, DRA Laboratory
- [14] Sound Intensity, a booklet by Bruel & Kjaer, Revision September 1993, 2850 Naerum, Denmark.
- [15] Stereophile magazine. Ohm Walsh 5 loudspeaker (review by Dick Olsher, June 1987), <http://www.stereophile.com/floorloudspeakers/687ohm/>
- [16] A Rouette, *Design of a bending wave loudspeaker*. Chalmers University of Technology, Department of Applied Acoustics, Report E04-01, 2004 Gothenburg, Sweden.
- [17] Mingsian R. Bai, Bowen Liu, *Determination of optimal exciter deployment for panel speakers using the genetic algorithm*, J.Sound Vib. 269, 727!743 (2004).
- [18] Shen Xiaoxiang et al, *Modal Optimization of Distributed Mode Loudspeaker*, 118th Convention, May 2005, Barcelona, Spain





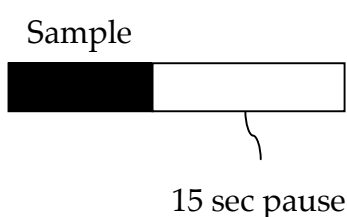


## Appendix A1. Questionnaire for listening test

# Listening Test

### Part I

In the first part of the test, you will hear several single sounds. Each sound will last 10 or 15 seconds. After that, there will be 15 seconds pause. Please answer the questions meanwhile.



Before moving forward to the practice of part I, please answer the following questions first.

**Do you have had any musical training, such as playing any kind of instrument and/or singing? If yes, please state what kind of training it is.**

No    Yes, \_\_\_\_\_

**Do you have any hearing impairment? If yes, please state your condition.**

No    Yes, \_\_\_\_\_

**Age:** \_\_\_\_\_

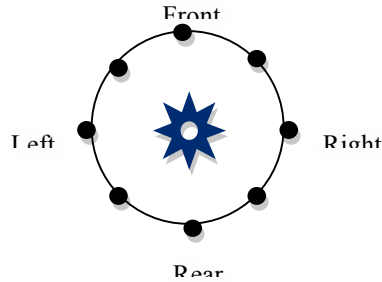
**Gender:** \_\_\_\_\_

**Nationality:** \_\_\_\_\_

### Practice

**Let's start with a sample sound. This is a sample sound that you will hear in Part I of the test. Please answer the questions after listening to the sound.**

- Can you locate the sound source? Please circle the black dot corresponding to the direction of the sound source which you feel. The sun in the middle represents your position. If you cannot locate it, please make a cross on the figure. (Choose the left only if you feel it is absolutely left. This also applies for right, front, and rear. If you feel the sound seems from the front but also could be from the left, choose the dot at left-front.)



- Do you feel it is clear? Please scale the clarity.

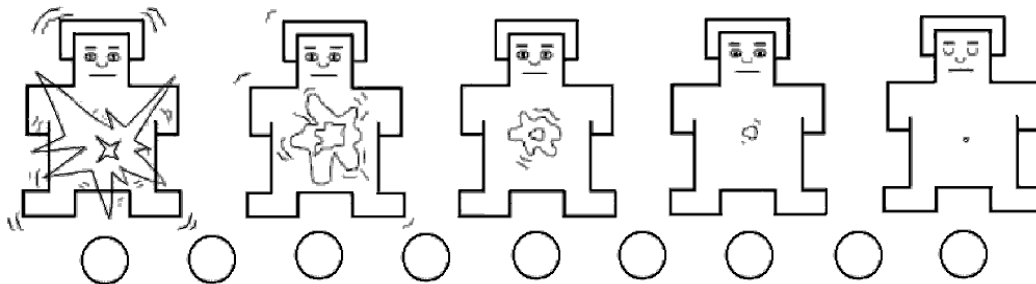
Very unclear                      Fair                      Very clear  
 0   1   2   3   4   5   6   7   8   9   10

- Do you feel anything not belong to the music itself? Please scale how loud they are.

None                      Acceptable                      Extremely loud  
 0   1   2   3   4   5   6   7   8   9   10

- How much do you feel you are activated or excited?

Very activated                      Fairly activated                      Not at all  
 (Very excited)                      (Fairly excited)                      (Not at all)



- How do you like it?



## Appendix A.2. Information of subjects

Nationality	Taiwanese	Mexican	Swedish	Italian	Chinese	Malaysian	French	German
Number of Subjects	5	1	5	1	4	2	1	1
Percentage of total subjects	25%	5%	25%	5%	20%	10%	5%	5%

**Table A.1 The nationalities of subjects**

Ages	20	21	22	23	24	25	26	28	29	30
Number of Subjects	1	1	1	1	5	4	3	1	1	2
Percentage of total subjects	5%	5%	5%	5%	25%	20%	15%	5%	5%	10%

**Table A.2 The ages of subjects**

Genders	Female	Male
Number of Subjects	10	10
Percentage of total subjects	50%	50%

**Table A.3 The genders of subjects**

Musical training	Yes	No
Number of Subjects	10	10
Percentage of total subjects	50%	50%

**Table A.4 Musical training**

## Appendix B. Equipment list

### B1. The test of material properties (ref 4.2)

Equipment & Type	Function
Complex Modulus Apparatus Type 3340	Resonance excitation and receiving
Integral amplifier	Magnifying the signal
MLSSA Ver. 10 rev9	Signal generator and receiver

**B2. The test of impulse response, frequency response, directivities, sensitivity, and distortions.**

Equipment & Type	Function
Sample DML from NXT	Sound source
Conventional loudspeaker from Apple	Sound source
Integral amplifier	Magnifying the signal
Microphone	Pick up the sound pressure
MLSSA Ver. 10 rev9	Signal generator and receiver
Turntable (only for directivities)	Rotate the loudspeakers to measure the impulse response at every angel
Anechoic chamber at Applied Acoustic Division in Chalmers	Provide a anechoic surrounding

**B3. Diffuse method for radiated sound power**

Equipment & Type	Function
Microphone	Pick up the sound pressure
Integral amplifier	Magnifying the signal
MLSSA Ver. 10 rev9	Signal generator and receiver
Calibrator	Calibrate the microphone

Sample DML from NXT	Sound source
Conventional loudspeaker from Apple	Sound source
Omni-directional sound source	Sound source for reverberation time measurement
Reverberation room	Provide the reverberant surrounding

#### **B4. The intensity method for radiated sound power**

Equipment & Type	Function
Paired microphone	Pick up the sound pressures
Integral amplifier	Magnifying the output signal
Trigger Happy on Acquisition Station VI	Signal generator and receiver
Cage	Define the mesh for sweeping
Sample DML from NXT	Sound source
Conventional loudspeaker from Apple	Sound source
Calibrator	Calibrate the microphone

#### **B5. The test of sound pressure level distribution**

Equipment & Type	Function
Microphone	Pick up the sound pressures
Integral amplifier	Magnifying the output signal
MLSSA Ver. 10 rev9	Signal generator and receiver

Sample DML from NXT	Sound source
Conventional loudspeaker from Apple	Sound source
Calibrator	Calibrate the microphone
Dummy head and torso	To estimate the effect of human's body and head (only used for paired impulse response measurement)

### **B6. The test of mechanical impedance and diaphragm scan**

Equipment & Type	Function
Accelerometer	Pick up the acceleration
Charge amplifier	Convert the signal from accelerometer to make it feasible
Integral amplifier	Magnifying the output signal
Trigger Happy on Acquisition Station VI	Signal generator and receiver
LDV	Signal generator and receiver
Sample DML from NXT	Vibrating surface



# Appendix C. Matlab scripts

## C1. The Matlab script for length/width ratio simulation

```
clear all;close all;clc
%% comparison of the nodal density between the room and the beam's
bending
f=20:5:2e4;
w=2*pi*f;
rho=500;
L=0.2;
H=1.2e-2;
W=0.16;
I=H^3/12;
m=rho*H*W;

E=6e9;
B=E*I;
moden_bw=L./(2*pi*sqrt(w))*(m/B)^(1/4);

c0=343;
V=5.08*7.8*3.62;
moden_room=w.^2*V/(2*pi^2*c0^3);

figure (1)
loglog(f,moden_room,f,moden_bw)
legend('room modal density','beam modal density')

%% find out the best ratio between the height and length with given
surface area
A=0.2*0.17;
NN=100;
na=50;
a=linspace(1/NN,1,NN);
lx=sqrt(A./a);
ly=lx.*a;
m=1:na;
n=1:na;
for mx=1:na
mn(na*(mx-1)+1:na*mx,:)= [m(mx)*ones(na,1) n'];
end

moden_n=zeros(na^2,NN);
for nxy=1:NN

        fn(:,nxy)=1/(2*pi)*sqrt((B/rho/H).*((mn(:,1)-
1)*pi/lx(nxy)).^2+((mn(:,2)-1)*pi/ly(nxy)).^2));
        ftemp=unique(fn(:,nxy));
        ntemp=length(ftemp);
        n_index(nxy)=ntemp-1;
        ffn(1:ntemp,nxy)=ftemp;
        difft(nxy)=sum(diff(ftemp).^2);
        if nxy==1
        moden_n(1:ntemp-2,nxy)=(1:ntemp-2)'./ftemp(2:end-1);
        avg_moden(nxy)=mean(moden_n(:,nxy));
        var_f(nxy)=var(ftemp);
        else
        moden_n(1:ntemp-1,nxy)=(1:ntemp-1)'./ftemp(2:end);
        avg_moden(nxy)=mean(moden_n(:,nxy));
        var_f(nxy)=var(ftemp);
```

```

end

end
[B_dff nt]=min(difft);
ni=find(avg_moden==max(avg_moden));
nmin=find(var_f==min(var_f));
[B_avg_modal xi]=sort(avg_moden,'descend');
[B_var_f xmin]=sort(var_f);
nbi=find(xi+xmin==min(xi+xmin));
['maximum moden density is ' num2str(avg_moden(ni)) '[1/Hz]']
['For the maximum average modal density, the best ratio is ('
num2str(a(ni)) ')'] ]
['For the most evenly modes distribution, the best ratio is ('
num2str(a(nmin)) ')'] ]
['For average modal density and evenly modes distribution, the best
ratio is (' num2str(a(nbi)) ')'] ]
%%
a60=find(abs(a-0.6)<1/NN/2);
a80=find(abs(a-0.8)<1/NN/2);
a100=find(abs(a-1)<1/NN/2);
a95=find(abs(a-45.8/48.3)<1/NN/2);
a40=find(abs(a-0.4)<1/NN/2);

figure (2)
plot(ffn(1:n_index(ni),ni),1:n_index(ni),'-
',ftemp(2:end),1:n_index(a100),'--
',ffn(1:n_index(a40),a40),1:n_index(a40),':',ffn(1:n_index(a60),a60),
1:n_index(a60),'-.',ffn(1:n_index(a80),a80),1:n_index(a80),'-
',ffn(1:n_index(a95),a95),1:n_index(a95),'-.','linewidth',2)
set(gca,'fontsize',16)
legend(['best, ratio='
num2str(a(ni))'],'ratio=1','ratio=0.4','ratio=0.6','ratio=0.8','gloden
ratio','Location','West')
xlabel('Nature frequencies [Hz]')
ylabel('Numbers of modes')
xlim([0 2e3])

figure (3)
plot(ffn(1:n_index(ni),ni),moden_n(1:n_index(ni)),ftemp(2:end),moden_
n(1:n_index(a100)),ffn(1:n_index(a60),a60),moden_n(1:n_index(a60)),ff
n(1:n_index(a80),a80),moden_n(1:n_index(a80)),ffn(1:n_index(a95),a95)
,moden_n(1:n_index(a95)))
legend('best','a=1','a=0.6','a=0.8','gloden ratio','Location','West')

%% the nature frequency and the modal density
load('nature_freq.mat');
N=1:1:length(fxy);
moden=N./fxy;

figure (4)
semilogx(fxy,moden)
xlabel('Nature frequency [Hz]')
ylabel('Modal density [1/Hz]')
xlim([20 2e4])

figure (5)
semilogx(N,fxy)
xlim([20 2e4])
ylabel('Nature frequency [Hz]')
xlabel('Number of modals [-]')

```

## Appendix D. Photos

D1. The Mobile Distributed Mode Loudspeaker “Yorozu Sound Revolution Universal Speaker Kit” used for the front cover was produced in Japan ca 2008.



**Figure D1. The Mobile Distributed Mode Loudspeaker**

D2. The setup for stereo impulse response



**Figure D2. The head and torso used for stereo impulse response**



**Figure D3. The setup for stereo impulse response**

D3. The mechanical impedance



**Figure D4. The LDV**



**Figure D5. The force transducer**